Article

Discovery of KBD4466, a Selective TLR 7/8 Inhibitor, for the Treatment of Autoimmune Diseases

Yonghai Yuan, Yonggang Wei,* Zhilong Jia, Hongzhu Chu, Dejiang Kong, Feiquan Lei, Fei Ye, Xinying Qian, Jing Zhang, Xibing Zhou, Xinying Zhu, Zhiyong Li, Xueya Liang, and Wei Chen

Cite This: https://doi.org/10.1021/acs.jmedchem.5c00656
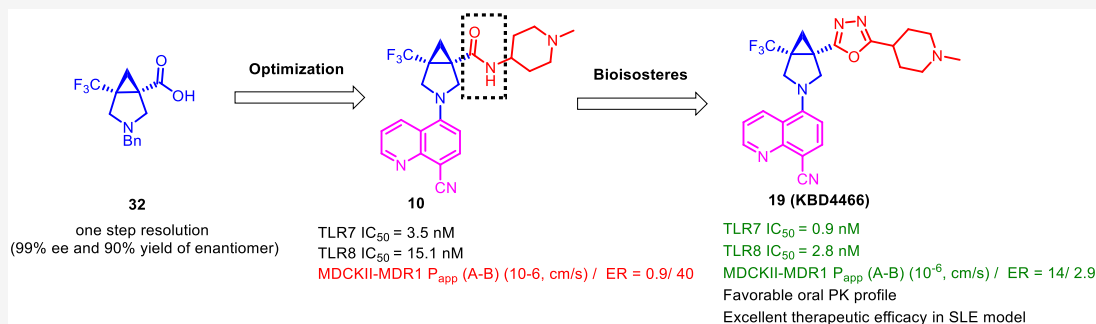
Read Online

ACCESS | Metrics & More | Article Recommendations | Supporting Information

ABSTRACT: The Toll-like receptor (TLR) family comprises a class of proteins that play a critical role in the innate immune system. Toll-like receptors TLR7 and TLR8 are transmembrane receptors that recognize single-stranded RNA. Aberrant activation of TLR7/8 is associated with the progression of certain autoimmune diseases, such as lupus. Therefore, highly selective inhibitors of TLR7/8 would be an effective therapeutic approach. Here, we have discovered a small molecule inhibitor, **KBD4466 (19)**, which demonstrates excellent cellular activity, favorable pharmacokinetic properties, potent inhibition of cytokine production in mouse pharmacodynamic studies, and outstanding therapeutic efficacy in an SLE animal model. Furthermore, we have developed an efficient synthetic route to access a [3.1.0] bicyclic system featuring chiral contiguous quaternary carbon centers.

INTRODUCTION

Toll-like receptors (TLRs) are vital receptors in the immune system, playing a central role in pathogen recognition and serving as essential components of the innate immune system. Their primary function is to identify pathogen-associated molecular patterns (PAMPs), positioning them within the broader category of pattern recognition receptors (PRRs).[1-3] TLR7 and TLR8 can recognize microbial single-stranded RNA, purine analogs, and imidazoquinolines, inducing the production of inflammatory cytokines and triggering immune responses to protect the host.[4,5] TLR7 is primarily expressed in monocytes, B cells, and plasmacytoid dendritic cells (pDCs), while TLR8 is predominantly expressed in neutrophils, monocytes, and myeloid dendritic cells. Although TLR7 and TLR8 share certain downstream signaling pathways, TLR7 activation preferentially engages the interferon regulatory factor (IRF) signaling cascade, leading to the production of type I interferons (IFNs). In contrast, TLR8 activation predominantly stimulates the nuclear factor-kappa B (NF-κB) pathway, resulting in the production of pro-inflammatory cytokines.[6,7] However, while TLR7 and TLR8 are involved in antiviral defense, their aberrant activation is potentially pathogenic and associated with the progression of certain autoimmune diseases such as lupus.[8,9] TLR7 has been identified as a key driver of lupus, supported by substantial genetic evidence from mouse models demonstrating its role in autoimmune diseases. Notably, TLR7 knockout (KO) significantly reduces lupus-like symptoms in murine models of systemic lupus erythematosus (SLE).[10-15] Similarly, dual knockout of TLR7 and TLR9 has demonstrated protective effects in murine models of SLE,[16,17] but surprisingly, TLR9 knockout alone exacerbated disease symptoms, raising questions about the relationship between TLR9 signaling and autoimmune diseases.[18,19] The role of TLR8 in mice is controversial, and compared to TLR7, there are fewer preclinical disease model data regarding its role in autoimmunity. However, studies have suggested that TLR8 expression correlates with disease in BXSB/MpJ-Yaa mice.[20-24] Additionally, in normal C57BL/6 mice, overexpression of TLR8 can trigger disease development.[25]
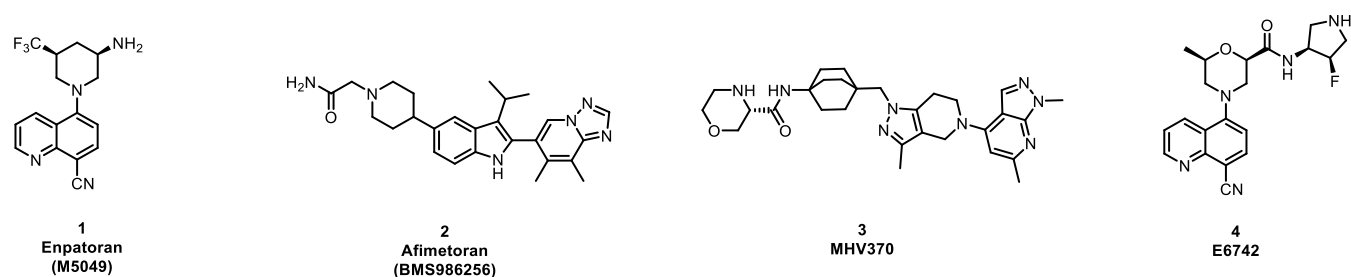
Figure 1. Chemical structures of TLR 7/8 antagonists in clinical development.

Therefore, selective inhibitors of TLR7/8 would be an effective therapeutic approach for treating SLE.

Currently, four small-molecule antagonists targeting TLR 7/8 are in clinical development (Figure 1).[26] The most advanced candidate, Merck's **M5049**, is undergoing multiple Phase II clinical trials for conditions including SLE and idiopathic inflammatory myopathies. Phase I studies have demonstrated that **M5049** exhibits favorable safety, tolerability, pharmacokinetics (PK), and pharmacodynamics (PD) profiles.[27−29] Similarly, Bristol Myers Squibb's TLR7/8 inhibitor **BMS986256** is currently in Phase II clinical trials for SLE. Phase I data indicate that **BMS986256** does not interfere with the metabolism of coadministered drugs, supporting its potential utility in combination therapies.[30,31] Additionally, Novartis' **MHV370**[32−34] and Eisai's **E6742**[35,36] are progressing in clinical trials. Moreover, several preclinical studies have been published,[37−39] further emphasizing the therapeutic potential of targeting TLR7/8 in the treatment of autoimmune diseases.

The application of all-carbon quaternary centers in drug development has garnered increasing attention, as their unique structure confers advantages in chemical stability, biological activity, and pharmacokinetics.[40−44] The high saturation and three-dimensional configuration of all-carbon quaternary centers can substantially enhance the metabolic stability of drug molecules.[45] In addition, these structures reduce the likelihood of enzymatic metabolism in vivo, thereby prolonging the drug's half-life. Furthermore, the incorporation of all-carbon quaternary centers into drug molecules may enhance specific binding interactions with target sites while minimizing interactions with off-target sites, consequently reducing adverse effects. Moreover, introducing quaternary centers enables the modulation of key physicochemical properties, such as solubility and permeability, thereby improving bioavailability.[46] However, the construction of all-carbon quaternary centers has long posed a significant challenge in organic synthesis and medicinal chemistry, particularly in cases involving consecutive adjacent quaternary carbon centers.[47−50] In this work, we designed and synthesized a [3,1,0] bicyclic system featuring adjacent quaternary carbon centers, which was subsequently applied to the development of TLR7/8 inhibitors.
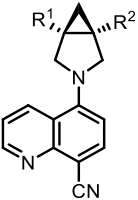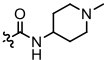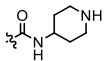
RESULTS AND DISCUSSION
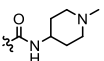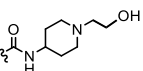
Compound **5** was initially designed and synthesized, but it demonstrated no cellular activity against TLR7 or TLR8 (Table 1). Replacing the carboxylic acid group with an amide to generate compound **6** did not result in a significant increase in TLR7/8 cellular activity. Notably, further derivatization of the amide to produce compound **7** led to a significant improvement in cellular activity, although additional optimization was still required. Substitution of the R[1] group with a trifluoromethyl moiety to yield compound **8** further enhanced

activity (compound **6** vs **8**). Subsequent derivatization of the amide to form compound **9** slightly reduced TLR7 activity but increased TLR8 activity. Excitingly, methylation of the piperidine to produce compound **10** resulted in satisfactory activity against both TLR7 and TLR8, while maintaining good selectivity for TLR9. However, compound **10** exhibited limitations, including poor permeability and significant cellular efflux. Substituting the methyl group with a hydroxyethyl group to generate compound **11** preserved activity, but the permeability showed no improvement. Replacing the piperidine ring w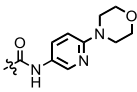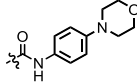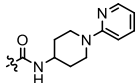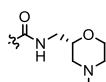ith an aromatic ring, as in compounds **12-14**, resulted in reduced TLR8 cellular activity, and altering the position of the aromatic ring in compound **15** produced similar outcomes. The introduction of a morpholine ring in place of the piperidine ring, as seen in compound **16**, improved permeability and reduced cellular efflux, albeit with a slight decrease in TLR8 cellular activity. Here, we observed that in the amide series, cellular activity and permeability are correlated with the basicity of the terminal fragment, exhibiting opposite trends. To achieve an optimal balance between cellular activity and permeability, compound **16** was selected as the lead compound for further investigation.

Crystal structures of TLR7 have been relatively scarce, whereas multiple crystal structures of TLR8 have been publicly disclosed.[51] The crystal structure of TLR8 (PDB ID: 7YTX) revealed the formation of a homodimeric complex, with two symmetrical binding pockets located at the interface between the monomers.[35] Through molecular docking analysis, several key interaction sites between compound **7** and TLR8 were revealed (Figure 2A). Specifically, the nitrogen atom in the quinoline ring forms a hydrogen bond with the Gly-351 residue, while the quinoline ring participates in π-π interactions with Phe-495*. Additionally, the protonated basic nitrogen atom within the piperidine ring establishes a strong salt bridge with the side chain of Glu-427. In comparison to compound **7**, compound **10** possesses an extra trifluoromethyl group that occupies a hydrophobic pocket (Figure 2C), thereby enhancing its binding affinity to TLR8 and resulting in improved cellular activity (Table 1, compound **7** vs **10**). In contrast, the secondary amine in the piperidine ring of compound **9** exhibits reduced basicity compared to that in compound **10**. This decrease in basicity weakens the salt bridge with the side chain of Glu-427 (Figure 2B), thereby resulting in reduced TLR8 cellular activity (Table 1, compound **9** vs **10**). Collectively, the molecular docking results suggest that the trifluoromethyl functional group and the basicity of the terminal nitrogen atom in the side chain play crucial roles in modulating TLR8 cellular activity. In light of these findings, further compound screening was undertaken to explore potential structure−activity relationships.

Table 1. Profiling Data of the Amide Series

Compound	R^1	R^2	TLR7 IC_{50} (nM)[a]	TLR8 IC_{50} (nM)[a]	TLR9 IC_{50} (nM)[a]	MDCKII-MDR1 P_{app} (A-B) (10^{-6}, cm/s) / ER^b
5	H	COOH	>10000	>10000	>10000	NT
6	H	$CONH_2$	>10000	>5000	>10000	NT
7	H		175 ± 2	92 ± 25	>10000	NT
8	CF_3		238 ± 16	1324 ± 306	>10000	NT
9	CF_3		286 ± 29	881 ± 53	>10000	NT
10	CF_3		3.5 ± 0.2	15.1 ± 2.2	>5000	0.9/ 40
11	CF_3		12.2 ± 2.1	41.2 ± 2.0	2768 ± 15	0.3/ 27
12	CF_3		31.9 ± 1.9	523 ± 23	>10000	NT
13	CF_3		17.0 ± 0.7	243 ± 12	>10000	NT
14	CF_3		8.9 ± 0.1	180 ± 1	>10000	NT
15	CF_3		19.1 ± 0.5	343 ± 43	>10000	NT
16	CF_3		16.5 ± 4.5	76.5 ± 3.4	>10000	7/ 5

[a]IC_{50} values in HEK293 cellular reporter assays for indicated TLRs are a mean of two or more individual determinations. [b]NT, not tested

In our aforementioned studies on amide-based compounds (Table 1), we identified molecules with promising TLR7/8 cellular activity. However, their further development was hindered by enduring permeability limitations that remained unresolved. To enhance the permeability and cellular activity of the compounds, we replaced the amide group with a 1,3,4-oxadiazole ring (Table 2). As bioisosteres of amides, 1,3,4-oxadiazole possesses favorable physicochemical properties and is commonly utilized in drug design.[52−55] Initially, we synthesized oxadiazole compound 17, which exhibited

C
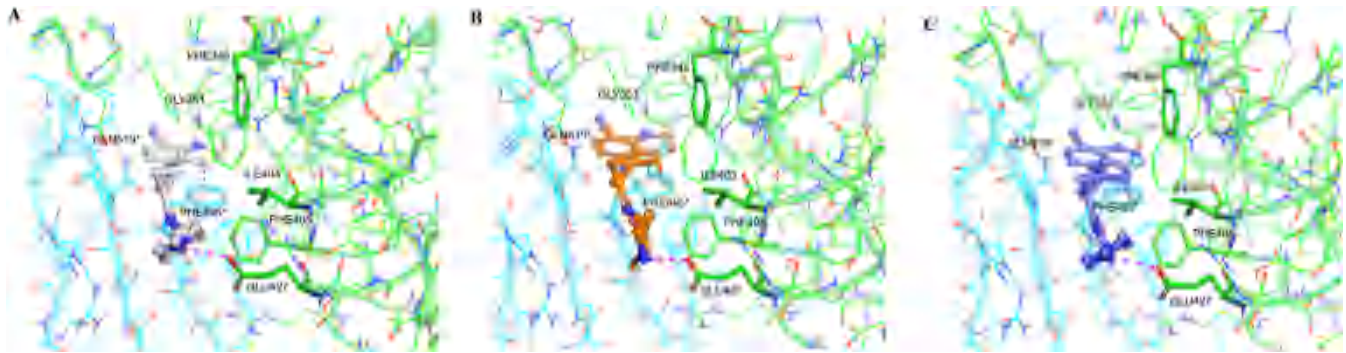
Figure 2. Molecular docking of **7**, **9**, **10** with TLR8 (PDB: 7YTX). (A) Docked model of **7** (white) bound to TLR8 (B) Docked model of **9** (orange) bound to TLR8. Trifluoromethyl moiety was positioned within a hydrophobic pocket. (C) Docked model of **10** (blue) bound to TLR8. The piperidine functional group within the molecule established a salt bridge with the side chain of Glu-427. Yellow dashed lines represented hydrogen bonds, blue dashed lines denoted π-π interactions, and pink dashed lines indicated salt bridges.

Table 2. Profiling Data of the 1,3,4-Oxadiazole Series

Compound	R^3	R^4	TLR7 IC$_{50}$ (nM)^a	TLR8 IC$_{50}$ (nM)^a	TLR9 IC$_{50}$ (nM)^a	MDCKII-MDR1 P$_{app}$ (A-B) (10^{-6}, cm/s) / ER^b
17			54.0 ± 0.4	107 ± 2	>10000	NT
18			74.9 ± 8.6	96.5 ± 13.2	>10000	NT
19 (KBD4466)			0.9 ± 0.3	2.8 ± 0.3	3024 ± 106	14/ 2.9
20			2.7 ± 0.1	7.5 ± 0.1	3179 ± 181	NT
21			4.3 ± 0.6	12.5 ± 1.4	4543 ± 276	NT
22			61.0 ± 7.4	63.2 ± 1.8	2886 ± 122	NT
23			1.1 ± 0.2	1.3 ± 0.2	>5000	NT
24			1356 ± 37	1375 ± 190	>10000	NT
25			33.9 ± 2.6	127 ± 17	>5000	NT

^{a}IC$_{50}$ values in HEK293 cellular reporter assays for indicated TLRs are a mean of two or more individual determinations. ^{b}NT, not tested

moderate cellular activity against TLR7/8 and demonstrated high selectivity for TLR9. Substituting the primary amine with an N-methylmorpholine group to produce compound **18** did not lead to further improvements in cellular activity. Notably, replacing the amino group with N-methylpiperidine to generate compound **19** (**KBD4466**) significantly enhanced TLR7/8 activity to the nanomolar range, accompanied by favorable permeability data. Compared to compound **10**, compound **19** exhibited improved TLR7/8 cellular activity, significantly enhanced permeability, and reduced efflux ratio, effectively addressing the challenge of balancing cellular activity and permeability observed in the amide series. The incorporation of a 1,3,4-oxadiazole ring conferred substantial drug-like benefits to the molecule. Based on the structural framework of **KBD4466**, we modified the quinoline moiety to yield compounds **22**, **24**, and **25**, each of which exhibited diminished cellular activity. Conversely, compounds **20**, **21**, and **23** retained their cellular potency, thereby justifying further pharmacodynamic (PD) studies to assess their efficacy.

Molecular docking analysis of compound **19** revealed that the binding pocket for this small-molecule inhibitor is situated at the interface between the two TLR8 protomers (Figure 3).
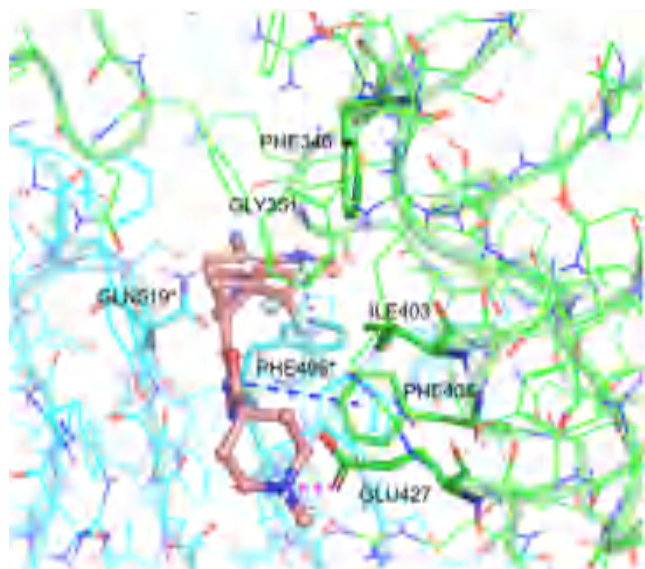

Figure 3. Molecular docking of **19** with TLR8 (PDB: **7YTX**). The piperidine functional group within the molecule established a salt bridge with the side chain of Glu-427. Yellow dashed lines represented hydrogen bonds, blue dashed lines denoted π-π interactions, and pink dashed lines indicated salt bridges.

Consistent with the docking results described above for compound **10**, a key interaction was identified, where a hydrogen bond forms between the basic nitrogen atom of the quinoline ring in compound **19** and the Gly-351 residue of TLR8. Furthermore, the quinoline ring of compound **19** engages in π−π stacking interactions with the Phe-495* residue. Moreover, the trifluoromethyl group was positioned within a hydrophobic pocket, while the terminal piperidine group significantly modulated TLR8 activity through interactions with the Glu-427 residue. Additionally, the 1,3,4-oxadiazole ring exhibits T-shaped π−π interactions with the Phe-405 residue. The T-shaped π−π interaction, also known as an edge-to-face interaction, was a significant noncovalent force between aromatic rings, playing a crucial role in drug design.

By modulating T-shaped π−π interactions, researchers optimized drug activity and selectivity.[56,57] Notably, in compound **19**, the introduction of an additional T-shaped π−π interaction was associated with enhanced cellular activity. Collectively, these interactions elucidated the influence of structural modifications on TLR8 activity and underscored the critical interactions that contributed to the high cellular activity of compound **19** against TLR8. The molecular docking analysis of compound **19** with TLR7 was included in the Supporting Information.

Based on the compounds identified in the above screening, additional pharmacodynamics (PD) experiments were conducted to further evaluate their potential therapeutic efficacy. Resiquimod (R848), a dual TLR7/8 agonist, was employed as a stimulus to robustly induce the production of the pro-inflammatory cytokine interleukin-6 (IL-6). The suppression of the R848-induced immune response was utilized as a pharmacodynamic (PD) assessment model in mice. In these PD experiments, several compounds (**16**, **18-21**, **23**) demonstrated significant inhibitory effects on IL-6 production. Among them, compounds **16**, **19**, and **23** exhibited inhibition rates exceeding 99%, highlighting their remarkable anti-inflammatory activity (Table 3).

Table 3. In Vivo Efficacy of 16, 18, 19, 20, 21, 23[a]

compd.	16	18	19	20	21	23
% inhibition of IL-6	99.7	94.9	99.4	86.0	96.4	99.4

[a]The R848-challenged mouse model was used for the in vivo efficacy study. Mice were given a single oral administration of compounds **16**, **18**, **19**, **20**, **21**, and **23** at 1 mg/kg, and 1 h later were dosed intraperitoneally (i.p.) with 25 μg of R848 per mouse. Blood samples were collected 2 h after R848 challenge, and IL-6 levels were measured by ELISA. The percent inhibition of cytokine release was calculated relative to mice dosed with R848 alone.

Following the acquisition of promising pharmacodynamic data, the pharmacokinetic profiles of compounds **16**, **19**, and **23** were evaluated in both mice and rats (Table 4). Although

Table 4. Mouse and Rat PK Profiles of 16, 19, 23[a]

	16		19		23	
	mouse	rat	mouse	rat	mouse	rat
P.O.: dose (mg/kg)	10	5	10	5	10	5
$T_{1/2}$ (h)	1.5	3.8	3.6	5.1	1.3	4.3
C_{max} (ng/mL)	1433	236	1297	948	595	415
AUC_{0-t} (ng·h/mL)	2954	1626	6247	7682	934	3138
% F	55	75	58	>99	43	86

[a]Formulation for i.v.: DMSO/30%HP-β-CD (10:90,v/v), p.o.: 0.5% MC.

Compound **23** exhibited favorable cellular activity, its plasma exposure (AUC_{0-t}) remained relatively low. Among these, compound **19** demonstrated superior pharmacokinetic properties, including high in vivo exposure and excellent bioavailability. Based on these findings, compound **19** was identified as the lead candidate for further pharmacodynamic evaluation.

In the pharmacodynamic (PD) efficacy study, **KBD4466** (**19**) and **M5049** were administered at a dose of 1 mg/kg at different time points (1, 4, 8, 16, and 24 h) prior to the R848 challenge (Figure 4). Interleukin-6 (IL-6) and interferon-α (IFN-α) play pivotal roles in the pathogenesis of systemic
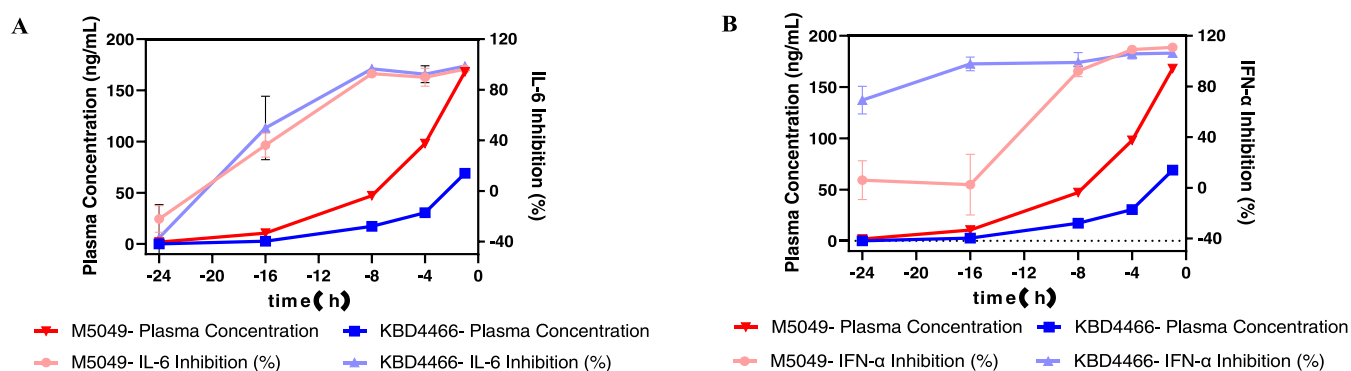
Figure 4. Pharmacodynamic effects in an R848-challenged mouse model. A time-course experiment was conducted in which mice received a single oral dose (1 mg/kg) of **KBD4466** (**19**) or **M5049**, followed by intraperitoneal (i.p.) administration of 25 μg R848 at predetermined intervals (24, 16, 8, 4, and 1 h postdosing). Blood samples were collected 2 h after R848 challenge for quantification of plasma compound concentrations and cytokine levels IL-6 (A) and IFN-α (B). The percentage inhibition of cytokine release was calculated relative to control mice treated with R848 alone.

lupus erythematosus (SLE). Through distinct immunomodulatory mechanisms, both cytokines contribute to disease progression and are commonly utilized as pharmacodynamic markers in therapeutic evaluations. In the **KBD4466** (**19**) treatment group, compared to the model group, IL-6 inhibition rates exceeded 50% at the 16-h time point and surpassed 90% at the 8-h time point (Figure 4A). In the multitime point study of IFN-α inhibition, **KBD4466** (**19**) exhibited superior efficacy in suppressing IFN-α compared to **M5049**, demonstrating a long-lasting inhibitory effect (Figure 4B). Specifically, at the 16-h time point, **KBD4466** (**19**) maintained a potent inhibitory effect on IFN-α with an inhibition rate of 98%, whereas M5049 achieved only a 2% inhibition rate. At the 24-h time point, **KBD4466** (**19**) continued to display remarkable IFN-α inhibitory activity, with an inhibition rate of 69%, compared to M5049's 6% inhibition rate. The observed relationship between drug concentration and the inhibition rates of IL-6 and IFN-α underscores a strong pharmacokinetic/pharmacodynamic (PK/PD) correlation. Notably, despite slightly lower plasma concentrations of **KBD4466** (**19**) compared to **M5049**, **KBD4466** (**19**) achieved comparable IL-6 inhibition and superior IFN-α suppression. This enhanced efficacy was likely attributable to the remarkable cellular activity of **KBD4466** (**19**).

As a candidate compound, **KBD4466** (**19**) was evaluated alongside **M5049** in a SLE model using BXSB/MpJ transgenic mice. Both compounds significantly improved survival rates compared to the model group, which exhibited a survival rate of 50% whereas the survival rate in the treated groups reached 100% (Figure 5A). Furthermore, both compounds significantly alleviated splenomegaly (Figure 5B) and lymphadenopathy (Figure 5C) while reducing plasma levels of autoantibodies, including antihistone antibodies (Figure 5D), antiribosomal P (anti-RiboP, Figure 5E) and antidouble- stranded DNA (anti-dsDNA, Figure 5F). In Systemic Lupus Erythematosus, kidney involvement (such as lupus nephritis) is a common and severe complication. Urinary microalbumin (MALB), the urinary microalbumin-to-creatinine ratio (MALB/CREA), and urinary total protein (UTP) are critical indicators for assessing kidney damage. Notably, **KBD4466** (**19**) exhibited an enhanced capacity to reduce MALB, MALB/CREA, and UTP levels (Figure 5G−I), underscoring its potential as a therapeutic candidate for SLE. Moreover, **KBD4466** significantly ameliorates renal swelling in the model, as evidenced by detailed

experimental data and analyses provided in the Supporting Information.

Chemistry. As depicted in Scheme 1, compound **30** containing a 3-azabicyclo[3.1.0]hexane unit was synthesized efficiently on a 1 kg scale via a two-step sequence: TFA-catalyzed [2 + 3] annulation of commercially available ethyl 4,4,4-trifluoro-2-butynoate **27** with N-benzyl-1-methoxy-N-((trimethylsilyl)methyl)methanamine **28** provided the key intermediate ethyl 1-benzyl-4-(trifluoromethyl)-2,5-dihydro-1H-pyrrole-3-carboxylate **29**. Corey-Chaykovsky cyclopropanation of compound **29** using trimethylsulfoxonium iodide and t-BuOK in DMSO afforded compound **30**. Finally, hydrolysis of the ester group in compound **30** delivered the corresponding acid **31**.

As shown in Table 5, the chiral resolution of racemic acid **31** was attempted. First, the typical chiral primary amine (R)-(+)-1-phenylethylamine **33** was employed, yielding the desired product **32** in 38% yield and 70% ee. Notably, when sterically enhanced primary amines (R)-(+)-1-(1-naphthyl)ethylamine **34** and (R)-(+)-1-(2-naphthyl)ethylamine **35** were used as resolution reagents, the opposite configuration of the enantiomer was obtained, with values of −77% ee and −37% ee, respectively. To further improve enantioselectivity, cinchonidine **36**, quinidine **37**, and substituted ethanolamines (**38**-**39**) were investigated. Gratifyingly, the substituted ethanolamine (1R,2S)-2-amino-1,2-diphenylethanol **39** gave significantly improved results (45% yield, 99% ee), approaching the theoretical maximum yield of 50% for an optically pure compound. This streamlined and effective resolution strategy established a robust foundation for the subsequent synthesis of the target compound.

The absolute configuration of compound **32** was determined through a four-step transformation of compound **32** to **43**. As shown in Scheme 2, the reaction of acid **32** with $SOCl_2$ in methanol led to ester **40**. Deprotection of the benzyl group for compound **40** under hydrogenation conditions gave amine **41**. Subsequently, N-Tosylation of compound **41** with p-toluenesulfonyl chloride and Et_3N afforded compound **42**. Finally, hydrolysis of the ester group in **42** provided acid **43**, whose absolute configuration was unambiguously established by X-ray crystallographic analysis (CCDC 240941 contains the supplementary X-ray crystallographic data of **43**; for details, see the Supporting Information).
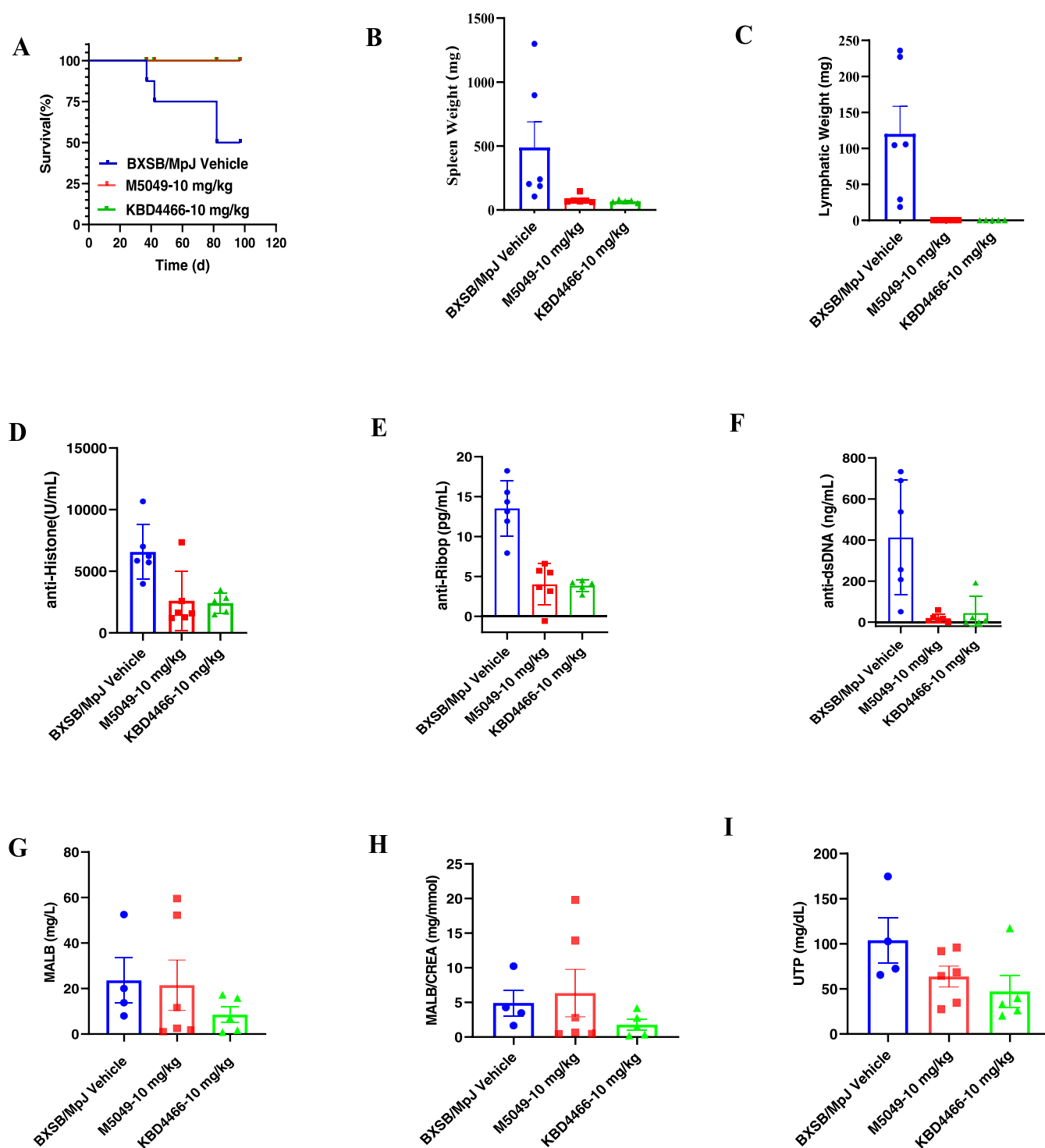
F

Figure 5. KBD4466 (**19**) efficacy in the BXSB/MpJ murine lupus model. Treatment with **KBD4466** (**19**) or **M5049** (QD) was initiated in BXSB/MpJ mice at 10 weeks of age via oral gavage. Survival rates were monitored (**A**). At end point, mice were sacrificed, spleen and lymph node weights were measured (**B**, **C**). Plasma were collected at the end point, antihistone antibodies (**D**), antiribosomal protein P antibodies(**E**), and anti-dsDNA antibodies(**F**) were quantified by ELISA. Urine collected at week 13 was analyzed for microalbumin (MALB, **G**), microalbumin-to-creatinine ratio (MALB/CREA, **H**), and total urinary protein (UTP, **I**).

As illustrated in Scheme 3, the synthesis of compounds **5-7**, featuring a noncontiguous quaternary carbon center, commenced with the commercially available compound **44**. Methylation of **44** under acidic conditions using $SOCl_2$ in MeOH produced compound **45**, followed by Buchwald-Hartwig coupling with 5-bromoquinoline-8-carbonitrile **46** using RuPhos Pd G3 as the catalyst, Cs_2CO_3 as the base, and

1,4-dioxane as the solvent, providing intermediate **47**. Treatment of **47** with $LiOH \cdot H_2O$ in THF/H_2O (4:1) converted it to carboxylic acid **5**. Subsequently, an efficient amide condensation of **5** with ammonium hydroxide (or 1-methylpiperidin-4-amine) in the presence of HATU and DIPEA in DMF afforded the corresponding compounds **6** and **7**. Starting from the intermediate **41**, compounds **8-16**
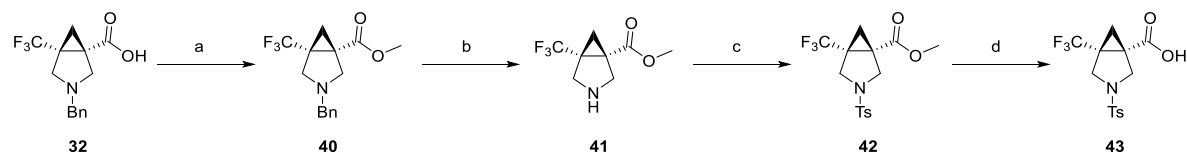
Scheme 1. Synthesis of Compound 31
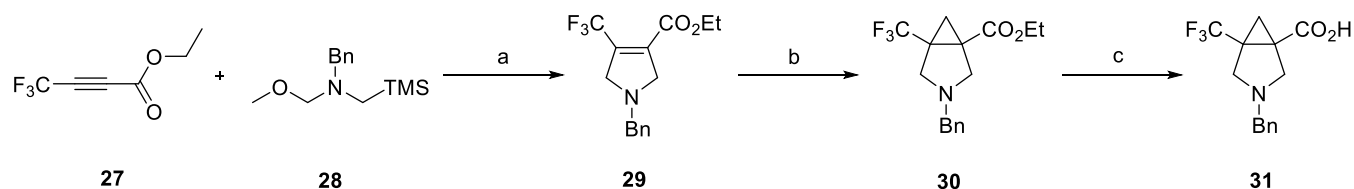
Reagents and conditions: (a) TFA, CH$_2$Cl$_2$, 0 °C to rt; (b) Trimethylsulfoxonium iodide, t-BuOK, DMSO, 0 to 60 °C; (c) LiOH·H$_2$O, THF/H$_2$O/CH$_3$OH = 10/10/1, 60 °C.

Table 5. Chiral Resolution of 31[a]

Resolution reagent	33	34	35	36	37	38	39
Structure							
yield(%)	38	30	63	32	0	0	45
ee (%)	70	−77	−37	75	−	−	99

[a]Reagents and conditions: 31(1.0 equiv), resolution reagent (1.0 equiv), EtOAc, rt to 80 °C.

Scheme 2. Synthesis of Compound 43

CCDC:2409641

Reagents and conditions: (a) SOCl$_2$, MeOH, 0 °C to reflux; (b) 10% Pd/C, H$_2$, MeOH, rt; (c) p-toluenesulfonyl chloride (p-TsCl), Et$_3$N, CH$_2$Cl$_2$, rt; (d) LiOH·H$_2$O, THF/H$_2$O = 4/1, 60 °C;

were synthesized using a similar approach to that adopted for the synthesis of compounds 6 and 7, as described earlier.

The synthesis of compounds 17-25 is described in Scheme 4. The synthesis of compounds 17-21 commenced with the above-obtained compound 48. Subjecting 48 to 2 equiv of N$_2$H$_4$·H$_2$O in MeOH afforded the hydrazide intermediate 50. Thereafter, compounds 17-21 were obtained through HATU (or POCl$_3$)-mediated amide coupling with corresponding carboxylic acids and subsequent cyclization. The synthesis of compounds 22-25 commenced with the above-obtained 32. A two-step sequence in one pot involving HATU-mediated amide condensation with 1-methylpiperidine-4-carbohydrazide 51 and subsequent cyclization by Burgess reagent smoothly converted 52 to 53. Removal of the N-Benzyl group of 53 readily produced the amine 54, followed by Pd-catalyzed Buchwald-Hartwig coupling reactions to furnish compounds 22-25.

◼ CONCLUSIONS

Aberrant activation of TLR7/8 receptors plays a pivotal role in the pathogenesis of various autoimmune diseases, including arthritis, psoriasis, and systemic lupus erythematosus (SLE). This underscores the therapeutic potential of developing TLR7/8 inhibitors as a strategy to treat autoimmune disorders. Quaternary carbon centers, with their unique stereochemical properties, are widely utilized in drug development to enhance pharmacological activity, improve metabolic stability, optimize physicochemical properties, and increase binding affinity to specific targets. In this study, we developed a synthetic method for [3,1,0] bicyclic compounds incorporating consecutive quaternary carbon centers, and optimized a chiral resolution process to efficiently produce the optically pure intermediate 32. Building upon this intermediate, we synthesized a series of small-molecule TLR7/8 inhibitors. Structure−activity relationship (SAR) analysis and structure-based drug design (SBDD) facilitated the identification of compounds with potent cellular TLR7/8 inhibitory activity. Further optimization of physicochemical properties led to the discovery of KBD4466 (19), a candidate compound exhibiting excellent drug-like properties. KBD4466 (19) demonstrated favorable pharmacokinetic (PK) profiles and sustained inhibitory effects on the inflammatory cytokines IL-6 and IFN-α in pharmacodynamic

Scheme 3. Synthesis of Compound 5−16
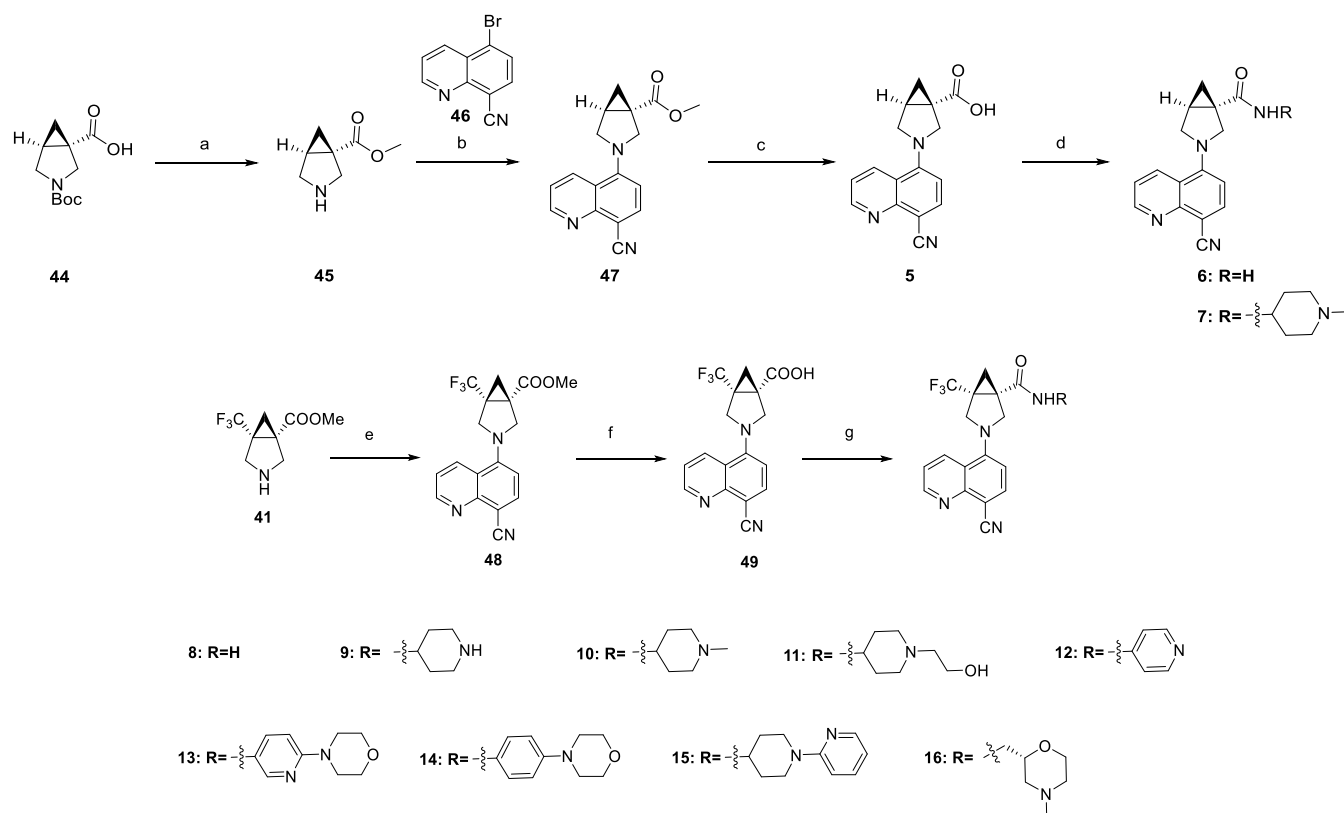
Reagents and conditions: (a) SOCl$_2$, MeOH, 0 °C to reflux; (b) 5-bromoquinoline-8-carbonitril, Ruphos Pd G3, Cs$_2$CO$_3$, 1,4-dioxane, 80 °C; (c) LiOH·H$_2$O, THF/H$_2$O =4/1, 60 °C; (d) R-NH$_2$, HATU, DIPEA, DMF, rt. (e) 5-bromoquinoline-8-carbonitrile, RuPhos Pd G3, Cs$_2$CO$_3$, 1,4-dioxane, 80 °C; (f) LiOH·H$_2$O, THF/H$_2$O =4/1, 60 °C; (g) R-NH$_2$, HATU, DIPEA, DMF, rt.

Scheme 4. Synthesis of Compound 17−25
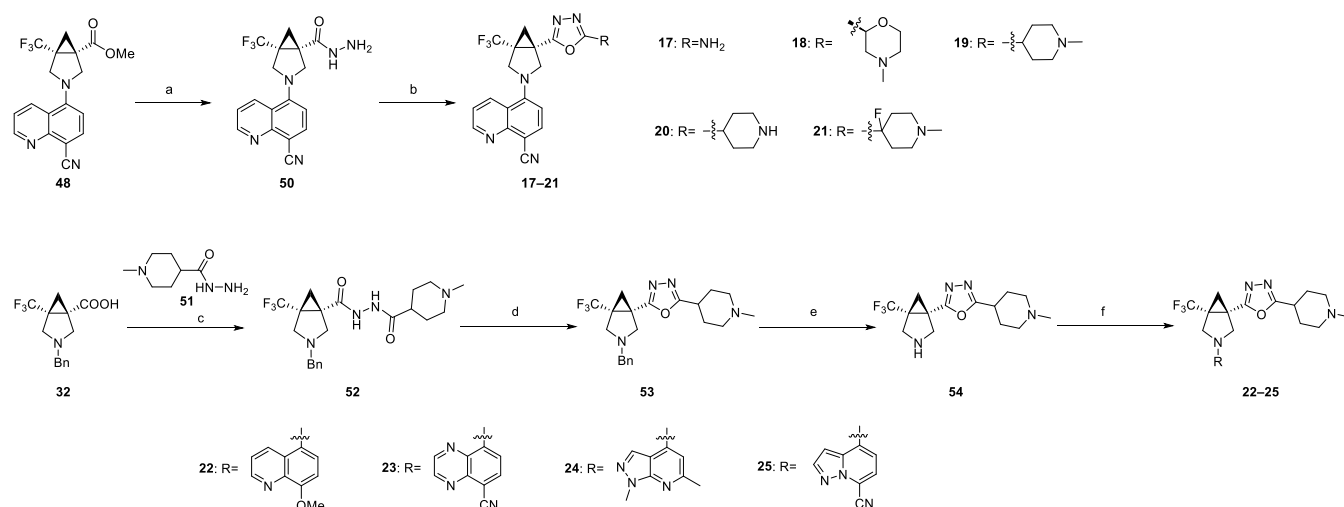
Reagents and conditions (a) N$_2$H$_4$·H$_2$O, CH$_3$OH, 85 °C; (b) R-COOH, substituted aniline, HATU, DIPEA, DMF, rt, then, Burgess reagent, rt. (c) HATU, DIPEA, DMF, rt; (d) Burgess reagent, rt; (e) 10% Pd/C, H$_2$, MeOH, rt; (f) R-Br or R-Cl, RuPhos Pd G3, Cs$_2$CO$_3$, 1,4-dioxane, 80 °C.

(PD) models. In the BXSB/MpJ mouse model of SLE, **KBD4466 (19)** significantly ameliorated disease progression and improved survival rates, highlighting its potential as a therapeutic agent for autoimmune diseases. Ongoing studies aimed at further evaluating **KBD4466 (19)** as a clinical candidate will be reported in due course.

■ EXPERIMENTAL SECTION

HEK-Blue hTLR7/8/9 Cell Assay. HEK-Blue hTLR7 cells, HEK-Blue hTLR8 cells, and HEK-Blue hTLR9 cells (InvivoGen) were seeded in black 384-well plates (Corning) with HEK-Blue Detection (InvivoGen). Test articles of different concentrations were added into plates for 30 min before stimulation of TLR7/8 agonist R848 (MCE) or the TLR9 agonist ODN2006 (InvivoGen). Cells were incubated for 16 h at 37 °C under 5% CO$_2$ atmosphere. The corresponding OD

values were obtained by Envision 2105 Multilabel Reader (PerkinElmer) at 620 nm, and the IC_{50} values of the compounds were calculated by Graphpad Prism 8.

MDCKII-MDR1 Permeability. MDCKII-MDR1 cells were plated into the transwell and cultured for 3−8 days under 37 °C, 5% CO_2 atmosphere. Cell monolayer integrity was assessed by transepithelial electrical resistance (TEER) before permeability testing. For Papp (A-B) or Papp (B-A) testing, compounds were added into the transwell insert (apical compartment) or the receiver plate (basolateral compartment) wells correspondingly. 50 μL sample were immediately collected from apical compartment or basolateral compartment for initial drug concentration testing. Another 50 μL sample were collected from apical compartment or basolateral compartment for drug concentration testing after 2 h incubation. LC-MS was used for drug concentration analysis. Papp was calculated as the following equation: Papp = (Vacceptor/Area × time) × (drug concentration of acceptor after incubation/drug concentration of donor at initial point). Efflux ratio was determined as the following equation: Efflux ratio = Papp(B-A)/Papp(A-B). Papp is apparent permeability (cm/s × 10^{-6}). Vacceptor is the volume (in mL) in the acceptor well, Area is the surface area of the membrane (0.143 cm^2 for Transwell-96 Well Permeable Supports), time is the total transport time in seconds.

In Vivo Experiments and Human Sample Ethics. All animal experiments were performed following the protocols evaluated and approved by the Institutional Animal Care and Use Committee (IACUC) of Kangbaida (Sichuan) Biotechnology Co., Ltd. The studies adheres to the ARRIVE guidelines and follows the principles of the 3Rs (replacement, reduction, refinement). The specific ethics approval numbers for the respective studies were as follows: R848-challenged mouse model (20230210-02), pharmacokinetic studies in mice (20230324-07), pharmacokinetic studies in rats (20230324-08), and the BXSB/MpJ SLE mouse model (20230601-01). Animals were housed in a specific pathogen-free (SPF) facility under controlled conditions (temperature: 22 ± 1 °C, humidity: 50 ± 10%, 12-h light/dark cycle) with ad libitum access to standard chow and water. Euthanasia was conducted via CO_2 inhalation followed by cervical dislocation, in compliance with the AVMA Guidelines for the Euthanasia of Animals. Human peripheral blood mononuclear cells (PBMCs) were sourced from healthy volunteers with informed consent from all participants. The collection and processing of these cells were conducted in accordance with the ethical approval granted by Shanghai Liquan Hospital Institutional Review Board (Ethics Approval Number: Z-ZJMS---21-10-001), and the cells were subsequently obtained from Milestone Biological Science & Technology Co., Ltd.

R848 Challenge Mouse Model. R848 challenge mouse model was used for pharmacodynamics or pharmacokinetic/pharmacodynamic study. For the pharmacodynamics study, female C57BL/6 mice (6−8 weeks old) were obtained from GemPharmatech. Mice were randomly divided into three groups (n = 6 per group): (1) Vehicle control (0.5% methylcellulose, MC+ saline); (2) R848 model (0.5% MC + R848); (3) Treatment (1 mg/kg compound in 0.5% MC + R848). The compound or vehicle was administered via oral gavage. One hour later, R848 (25 μg/mouse, dissolved in saline) was intraperitoneally injected into the model and treatment groups, while the vehicle group received saline alone. Blood samples were collected 2 h post-R848 challenge and centrifuged at 3000g for 10 min to isolate plasma. Quantification of IL-6 levels in plasma was performed using ELISA kit (Invitrogen) according to the manufacturer's protocol. The percentage inhibition was calculated as Inhibition (%) = [1 − (Ctreatment − Cvehicle)/(Cmodel − Cvehicle)] × 100, where C represents cytokine concentration. For pharmacokinetic/pharmacodynamic study, the experimental procedure was largely similar to the one described above with a few modifications. Specifically, mice were pretreated with the compound at 1, 4, 8, 16, and 24 h before R848 challenge (n = 5 per group). Blood samples were collected at each time point for plasma drug concentration analysis by LC-MS/MS and measurement of IFN-α and IL-6 levels by ELISA.

Pharmacokinetic Studies in Mice and Rats. Male ICR mice and male Sprague−Dawley (SD) rats (Charles River Laboratories) were used for Pharmacokinetic Studies. Animals were treated with compound **16**, compound **19**(**KBD4466**) or compound **23** via oral administration (0.5% methylcellulose) and intravenous injection (DMSO/30%HP-β-CD: 10/90(v/v)). Mice received doses of 10 mg/kg (p.o.) and 1 mg/kg (i.v.), while SD rats were dosed at 5 mg/kg (p.o.) and 1 mg/kg (i.v.). Each group consisted of three animals. Plasma was collected at different time points and compound concentrations were quantified by LC-MS/MS. Pharmacokinetic parameters were calculated using Phoenix WinNonlin software.

BXSB/MpJ SLE Mouse Model. Female BXSB/MpJ mice were obtained from Jackson Laboratories at 7 weeks of age. After a one-week acclimation period, treatments were initiated and continued for 14 weeks. Mice were orally administered 10 mg/kg **KBD4466** or **M5049** once daily, formulated in 0.5% methylcellulose (n = 6 per group). Survival was monitored throughout the study. Urine samples were collected at week 13, and microalbumin and creatinine levels were quantified. At the study end point, plasma samples were collected for autoantibody analysis. Spleens and cervical lymph nodes were excised and weighed. The spleen index was calculated as the ratio of spleen weight to body weight (milligrams/grams). Plasma autoantibodies, including antihistone antibodies (Creative Diagnostics, DEIA120J), antiribosomal protein P antibodies (JiNing Bio, JN20553), and anti-dsDNA antibodies (Creative Diagnostics, DEIA4488), were measured using the corresponding ELISA kits. OD values were recorded at 450 nm, and autoantibody concentrations were expressed as units per milliliter (U/mL).

Molecular Docking Study. AutoDock 4.2.6 was employed to perform molecular docking studies. The PDB structure of the target protein was initially prepared by importing it into AutoDock, where water molecules were removed, hydrogen atoms were added, and any missing residues were completed using MODELER. The grid box was defined based on the central coordinates of the cocrystallized ligand to ensure accurate docking. Docking simulations were conducted using the genetic algorithm to explore binding conformations. Finally, the protein−ligand interactions were visualized and analyzed using PyMOL.

Chemical Synthesis Procedures. Chemical analysis methods.^{1}**H NMR**, ^{13}**C NMR** and ^{19}**F NMR** spectra were recorded in $CDCl_3$, DMSO-d_6 or CD_3OD solution at Bruker Avance NEO 400 MHz instrument. Chemical shifts were denoted in ppm (δ) and calibrated by using residual undeuterated solvent ($CDCl_3$ = 7.27 ppm, DMSO-d_6 = 2.50 ppm, CD_3OD = 3.31 ppm), tetramethylsilane (0.00 ppm) as internal reference for ^{1}**H NMR** and the deuterated solvent ($CDCl_3$ = 77.00 ppm, DMSO-d_6 = 39.50 ppm, CD_3OD = 49.00 ppm) as internal standard for ^{13}**C NMR**. The following abbreviations were indicated as follows: s = singlet, d = doublet, t = triplet, m = multiplet, and dd = double doublet. High-resolution mass spectral analysis (**HRMS**) data were measured on a Thermo scientific Q Exactive Plus mass machine, The X-ray single-crystal determination was performed on an XtaLAB Synergy R X-ray diffractometer. Chiral HPLC was recorded on an Agilent 1260 Infinity II HPLC machine. The chiral stationary phases were Daicel Chiralpak AD columns (Ø = 0.46 cm, length = 25.0 cm). Analytical HPLC was recorded on a Agilent 1260 Infinity II HPLC machine, all final compounds were >95% purity.

General Procedure for the Synthesis of 32. *Ethyl-1-benzyl-4-(trifluoromethyl)-2,5-dihydro-1H-pyrrole-3-carboxylate (29).* To a stirred solution of **27** (1.00 kg, 6.02 mol) in 8 L of dichloromethane was added a trifluoroacetic acid (6.8 g, 0.06 mol) at 0 °C. A solution of **28** (1.43 kg, 6.02 mol) in dichloromethane (2 L) was then slowly added dropwise. The reaction mixture was stirred at room temperature for 2 h, then quenched with saturated aqueous sodium bicarbonate and extracted with dichloromethane. The organic layers were combined, washed with brine, dried by anhydrous sodium sulfate, filtered, and concentrated under reduced pressure to afford the compound **29** as yellow oil (1.70 kg). This crude mixture was used directly in the next step without further purification.

Ethyl-3-benzyl-5-(trifluoromethyl)-3-azabicyclo [3.1.0] hexane-l-carboxylate (30). An oven-dried round-bottom flask was charged

with potassium *tert*-butoxide (0.71 kg, 6.32 mol) and dimethyl sulfoxide (5 L). Trimethylsulfoxonium iodide (1.32 kg, 6.02 mol) in dimethyl sulfoxide (1 L) was added to the resulting suspension over a period of 10 min at 0 °C, and the reaction mixture was stirred at 0 °C for 30 min. Afterward, a solution of compound **29** in dimethyl sulfoxide (5 L) was added to the reaction mixture. The resulting reaction mixture was heated in an oil bath at 60 °C for 2 h, and then it was quenched with saturated aqueous ammonium chloride and extracted with dichloromethane. The organic layers were combined, washed with brine, dried over sodium sulfate, filtered, and concentrated under reduced pressure. The crude product was purified by flash column chromatography ($V_{\text{Petroleum ether}}/V_{\text{Ethyl acetate}}$ = 10:1) to afford product **30** (1.49 kg, 79% yield for two steps, colorless oil). ^{1}**H NMR** (400 MHz, CD$_3$OD) δ = 7.68 (s, 2H), 7.54−7.43 (m, 3H), 4.56 (s, 2H), 4.24 (q, J = 7.1 Hz, 2H), 4.16 (d, J = 11.5 Hz, 1H), 3.97 (d, J = 12 Hz, 1H), 3.88 (d, J = 12 Hz, 1H), 3.80 (d, J = 12 Hz, 1H), 2.38−2.20 (m, 2H), 1.27 ppm (t, J = 7.1 Hz, 3H). ^{13}**C NMR** (100 MHz, CD$_3$OD) δ = 166.67, 132.23, 131.45, 130.87, 130.37, 125.52 (q, J = 272 Hz, 1C), 63.60, 59.69, 56.22, 54.31, 38.13 (q, J = 36 Hz, 1C), 34.86, 17.68, 14.19 ppm. ^{19}**F NMR** (377 MHz, CD$_3$OD) δ = −64.63 ppm. **HRMS** (ESI) *m/z*: [M + H]$^+$ calcd for C$_{16}$H$_{19}$F$_3$NO$_2$ 314.1362; found: 314.1364.

3-Benzyl-5-(trifluoromethyl)-3-azabicyclo[3.1.0]hexane-1-carboxylic Acid (31). To a solution of compound **30** (1.49 kg, 4.76 mol) in THF/H$_2$O/CH$_3$OH = 10/10/1(5 L), lithium hydroxide (0.8 kg, 19.04 mol) was added. The reaction mixture was heated in an oil bath at 60 °C for 2 h. Then, 2N aqueous HCl was added, and the pH was adjusted to 3−4. The mixture was extracted with ethyl acetate. The organic layers were combined, washed with brine, dried by anhydrous sodium sulfate, filtered, and concentrated under reduced pressure to afford the compound **31**. This crude compound was used directly in the next step without further purification (1.1 kg, 81% yield, white solid).

(1S,5R)-3-Benzyl-5-(trifluoromethyl)-3-azabicyclo[3.1.0]hexane-1-carboxylic Acid (32). To a stirred solution of compound **31** (300 g, 1.05 mol) in 16.8 L of ethyl acetate, (1*R*,2*S*)-(−)-2-amino-1,2-diphenylethanol (224 g, 1.05 mol) was added at room temperature and stirred for 10 min. A large amount of white solid was precipitated. The mixture was heated to reflux, and ethyl acetate was added dropwise until the solution became completely clear. The solution was then cooled to room temperature, and the solid was filtered. The resulting solid was washed twice with a small amount of ethyl acetate and then dried to obtain the salt. This salt was dissolved in water, 4 N HCl aq was added, and the pH was adjusted to 3−4. The organic phase was separated, washed with brine, dried by anhydrous sodium sulfate, filtered, and concentrated under reduced pressure to afford the compound **32** (135 g, 45% yield, white solid, 99% *ee*). ^{1}**H NMR** (400 MHz, CDCl$_3$) δ = 13.25 (s, 1H), 7.37−7.32 (m, 5H), 4.08−4.00 (m, 2H), 3.53 (d, J = 10.4 Hz, 1H), 3.48 (d, J = 10.3 Hz, 1H), 3.40 (d, J = 10.3 Hz, 1H), 3.08 (d, J = 10.2 Hz, 1H), 2.03 (d, J = 10.1 Hz, 1H), 1.83 ppm (d, J = 4.5 Hz, 1H). ^{13}**C NMR** (100 MHz, CDCl$_3$) δ = 171.06, 133.87, 129.63, 128.67, 128.50, 124.69 (q, J = 272 Hz, 1C), 58.24, 55.63, 53.00, 36.83 (q, J = 36 Hz, 1C), 35.02, 16.25 ppm. ^{19}**F NMR** (377 MHz, CDCl$_3$) δ = −63.58 ppm. **HRMS** (ESI) *m/z*: [M + H]$^+$ calcd for C$_{14}$H$_{15}$F$_3$NO$_2$ 286.1049; found: 286.1049. The *ee* value was determined by the chiral HPLC analysis (Daicel Chiralpak AD, *n*-hexane/methanol = 95:5, v = 1 mL/min, λ= 214.0 nm; t_{minor} = 2.007 min, t_{major} = 2.582 min).

Screening of Chiral Resolution Agent. To a stirred solution of compound **31** (5 g, 17.5 mmol) in 50 mL of ethyl acetate, chiral amine (17.5 mmol) was added at room temperature, and the mixture was stirred for 10 min. A large amount of white solid precipitated. The mixture was heated to reflux, and ethyl acetate was added dropwise until the solution became completely clear. The solution was then cooled to room temperature, and the solid was filtered. The resulting solid was washed twice with a small amount of ethyl acetate and then dried to obtain the salt. This salt was dissolved in water, 4N aqueous HCl was added, and the pH was adjusted to 3−4. The organic phase was separated, washed with brine, dried over anhydrous sodium

sulfate, filtered, and concentrated under reduced pressure to afford compound **32**.

General Procedure for the Synthesis of 43 (CCDC 2409641) and Its X-ray Crystallographic Analysis. *Methyl (1S,5R)-3-Benzyl-5-(trifluoromethyl)-3-azabicyclo[3.1.0]hexane-1-carboxylate 40.* An oven-dried round-bottom flask was charged with compound **32** (50 g, 175 mmol) and methanol (1 L). Thionyl chloride (50 mL) was added dropwise via syringe over 15 min. The reaction mixture was heated in an oil bath at 60 °C for 2 h, then quenched with saturated aqueous sodium bicarbonate and extracted with ethyl acetate. The organic layers were combined, washed with brine, dried over anhydrous sodium sulfate, filtered, and concentrated under reduced pressure. The crude product was purified by flash column chromatography ($V_{\text{petroleum ether}}/V_{\text{ethyl acetate}}$ = 10:1) to afford product **40** (41.9 g, 80% yield, colorless oil). ^{1}**H NMR** (400 MHz, CD$_3$OD) δ = 7.73−7.62 (m, 2H), 7.52−7.43 (m, 3H), 4.61−4.51 (m, 2H), 4.17 (d, J = 11.5 Hz, 1H), 4.02−3.84 (m, 2H), 3.78 (s, 4H), 2.36−2.22 ppm (m, 2H). ^{13}**C NMR** (100 MHz, CD$_3$OD) δ = 167.14, 132.21, 131.45, 130.84, 130.37, 124.96 (q, J = 274 Hz, 1C). 59.73, 56.18, 54.29, 53.74, 38.20 (q, J = 38 Hz, 1C), 34.73, 17.72 ppm. ^{19}**F NMR** (377 MHz, CD$_3$OD) δ = −64.99 ppm. **HRMS** (ESI) *m/z*: [M + H]$^+$ calcd for C$_{15}$H$_{17}$F$_3$NO$_2$ 300.1206; found: 300.1207.

Methyl (1S,5R)-5-(Trifluoromethyl)-3-azabicyclo[3.1.0]hexane-1-carboxylate 41. The solution of compound **40** (41.9 g, 140 mmol) in methanol (1 L) was treated with palladium on carbon (10 wt %, 3.0 g, 19 mmol). The reaction mixture was stirred at room temperature for 12 h under a hydrogen balloon, follow by Celite filtration, then quenched with saturated aqueous sodium bicarbonate and extracted with dichloromethane. The organic layers were combined, washed with brine, dried by anhydrous sodium sulfate, filtered and concentrated under reduced pressure. The crude product was purified by flash column chromatography ($V_{\text{Petroleum ether}}/V_{\text{Ethyl acetate}}$ = 1:1) to afford product **41** (25.1 g, 86 yield, colorless oil). ^{1}**H NMR** (400 MHz, DMSO-d_6) δ = 10.31 (brs, 1H), 3.79 (d, J = 11.8 Hz, 1H), 3.70 (s, 3H), 3.69−3.58 (m, 3H), 2.16 (dd, J = 7.0, 1.3 Hz, 1H), 2.09 ppm (d, J = 7.0 Hz, 1H). ^{13}**C NMR** (100 MHz, DMSO-d_6) δ = 166.23, 124.01 (q, J = 272 Hz), 53.01, 47.25, 45.13(d, J = 8 Hz, 1C), 36.58 (q, J = 36 Hz, 1C), 33.60, 15.50 ppm. ^{19}**F NMR** (377 MHz, CDCl$_3$) δ = −62.82 ppm. **HRMS** (ESI) *m/z*: [M + H]$^+$ calcd for C$_8$H$_{11}$F$_3$NO$_2$ 210.0736; found: 210.0739.

Methyl (1S,5R)-3-Tosyl-5-(trifluoromethyl)-3-azabicyclo[3.1.0]hexane-1-carboxylate 42. To a solution of **41** (250 mg, 1.2 mmol) in dichloromethane was added triethylamine (0.5 mL, 3.6 mmol), and *p*-toluenesulfonyl chloride (343 mg, 1.8 mmol). The reaction mixture was stirred at room temperature for 2 h, and then quenched with saturated aqueous sodium bicarbonate and extracted with ethyl acetate. The organic layers were combined, washed with brine, dried by anhydrous sodium sulfate, filtered and concentrated under reduced pressure. The crude product was purified by flash column chromatography ($V_{\text{Petroleum ether}}/V_{\text{Ethyl acetate}}$ = 10:1) to afford the product **42** (260 mg, 60% yield, white solid). ^{1}**H NMR** (400 MHz, DMSO-d_6) δ = 7.74 (d, J = 8.3 Hz, 2H), 7.49 (d, J = 8.0 Hz, 2H), 3.76 (d, J = 9.9 Hz, 1H), 3.71 (dd, J = 10.0, 0.8 Hz, 1H), 3.63 (s, 3H), 3.42 (d, J = 10.0 Hz, 1H), 3.27 (d, J = 9.9 Hz, 1H), 2.42 (s, 3H), 1.98 (d, J = 6.2 Hz, 1H), 1.40−1.34 ppm (m, 1H). ^{13}**C NMR** (100 MHz, DMSO-d_6) δ = 166.58, 144.36, 132.09, 130.19, 127.56, 124.08 (q, J = 271 Hz, 1C), 52.77, 50.06, 48.19, 36.87 (q, J = 36 Hz, 1C), 33.85, 21.06, 16.08 ppm. ^{19}**F NMR** (377 MHz, DMSO-d_6) δ = −62.85 ppm. **HRMS** (ESI) *m/z*: [M + H]$^+$ calcd for C$_{15}$H$_{17}$F$_3$NO$_4$S 364.0825; found: 364.0832.

(1S,5R)-3-Tosyl-5-(trifluoromethyl)-3-azabicyclo[3.1.0]hexane-1-carboxylic Acid 43. To a solution of **42** (260 mg, 0.72 mmol) in THF/H$_2$O = 4/1(10 mL) was added lithium hydroxide (57.6 mg, 1.44 mmol). The resulting mixture was stirred vigorously at the 60 °C for 10 h. 2*N* HCl aq was added, and the pH was adjusted to 3−4, and extracted with ethyl acetate. The organic layers were combined, washed with brine, dried by anhydrous sodium sulfate, filtered, and concentrated under reduced pressure. The crude product was purified by flash column chromatography ($V_{\text{Dichloromethane}}/V_{\text{Methanol}}$ = 10:1) to afford the compound **43** (180 mg, 72% yield, white solid). ^{1}**H NMR**

(400 MHz, DMSO-d_6) δ = 13.40 (s, 1H), 7.74 (d, J = 8.3 Hz, 2H), 7.49 (d, J = 8.1 Hz, 2H), 3.74 (d, J = 9.9 Hz, 1H), 3.67 (d, J = 9.9 Hz, 1H), 3.39 (d, J = 9.9 Hz, 1H), 3.24 (d, J = 9.8 Hz, 1H), 2.42 (s, 3H), 1.94 (d, J = 5.9 Hz, 1H), 1.33 (d, J = 4.6 Hz, 1H). ^{13}**C NMR** (100 MHz, DMSO-d_6) δ = 167.77, 144.35, 131.96, 130.18, 127.61, 124.28 (q, J = 272 Hz, 1C), 50.34, 48.39, 36.63 (q, J = 36 Hz, 1C), 34.04, 21.07, 16.06. ^{19}**F NMR** (377 MHz, CDCl$_3$) δ = −62.50 ppm. **HRMS** (ESI) m/z: [M + H]$^+$ calcd for C$_{14}$H$_{15}$F$_3$NO$_4$S 350.0668; found: 350.0676. The single crystal of **43** (99% ee), which was recrystallized from petroleum ether and ethyl acetate ($V_{\text{Petroleum ether}}/V_{\text{Ethyl acetate}}$ = 5:1), was used for the determination of its absolute configuration via X-ray crystallography (see Supporting Information). The intensity data were collected on a XtaLAB Synergy R, DW system, HyPix diffractometer. The crystal was kept at 294.60(10) K during data collection. These data can be obtained free of charge via www.ccdc.cam.ac.uk/data_request/cif.

General Procedure for the Synthesis of Compounds 5−16. *Methyl (1S,5S)-3-(8-Cyanoquinolin-5-yl)-3-azabicyclo[3.1.0]-hexane-1-carboxylate 47.* An oven-dried round-bottom flask was charged with **44** (3.0 g, 13.2 mmol) and methanol (10 mL). Thionyl chloride (10 mL) was added via syringe dropwise over 15 min. The reaction mixture was heated in an oil bath at 60 °C for 2 h, and then quenched by saturated aqueous sodium bicarbonate and extracted with ethyl acetate. The organic layers were combined, washed with brine, dried by anhydrous sodium sulfate, filtered and concentrated under reduced pressure. The crude product was purified by flash column chromatography ($V_{\text{Dichloromethane}}/V_{\text{Methanol}}$ = 10:1) to afford the product **45** (1.7 g, 74% yield, white solid). Compound **45**, being a commercially available reagent, was directly employed in the subsequent reaction. To an oven-dried 50 mL round-bottom flask equipped with a stirring bar was added **45** (1.7 g, 9.6 mmol), 5-bromoquinoline-8-carbonitrile **46** (2.23 g, 9.6 mmol), cesium carbonate (9.38 g, 28.8 mmol), and dry 1,4-dioxane (20 mL). The resultant mixture was degassed three times, and then RuPhos Pd G3 (0.80 g, 0.96 mmol) was added to the above reaction mixture under argon atmosphere. The reaction mixture was heated in an oil bath at 80 °C for 3 h. The resulting solution was filtered. The solvent was extracted with ethyl acetate, washed with brine, dried by anhydrous sodium sulfate, filtered and concentrated under reduced pressure. The crude product was purified by flash column chromatography ($V_{\text{Petroleum ether}}/V_{\text{Ethyl acetate}}$ = 1:1) to afford the product **47** (1.5 g, 53% yield, white solid). ^{1}**H NMR** (400 MHz, CDCl$_3$) δ = 8.91 (d, J = 4.0 Hz, 1H), 8.33 (d, J = 8.6 Hz, 1H), 7.84 (d, J = 8.1 Hz, 1H), 7.37 (dd, J = 8.6, 4.2 Hz, 1H), 6.88 (d, J = 8.2 Hz, 1H), 3.81−3.70 (m, 3H), 3.69 (s, 3H), 3.44 (dd, J = 9.9, 3.7 Hz, 1H). 2.21−2.14 (m, 1H), 1.57 (dd, J = 8.1, 4.6 Hz, 1H), 1.39 ppm (t, J = 4.8 Hz, 1H).^{13}**C NMR** (100 MHz, CDCl$_3$) δ = 172.28, 151.50, 150.63, 148.92, 135.72, 133.12, 121.84, 120.29, 118.03, 111.78, 104.43, 53.10, 52.88, 51.87, 28.86, 26.44, 16.28 ppm. **HRMS** (ESI) m/z: [M + H]$^+$ calcd for C$_{17}$H$_{16}$N$_3$O$_2$ 294.1237; found: 294.1238.

(1S,5S)-3-(8-Cyanoquinolin-5-yl)-3-azabicyclo[3.1.0]hexane-1-carboxylic Acid 5. To a solution of **47** (1.5 g, 5.1 mmol) in THF/H$_2$O = 4/1(10 mL) was added lithium hydroxide (367 mg, 15.3 mmol). The resulting mixture was stirred vigorously at room temperature for 10 h. 2 N HCl aqueous solution was added, and the pH was adjusted to 3−4, and extracted with ethyl acetate. The organic layers were combined, washed with brine, dried by anhydrous Na$_2$SO$_4$, filtered, and concentrated under reduced pressure. The crude product was purified by flash column chromatography ($V_{\text{Petroleum ether}}/V_{\text{Ethyl acetate}}$ = 1:1) to afford product **5**. (1.3 g, 91% yield, white solid). ^{1}**H NMR** (400 MHz, DMSO-d_6) δ = 12.59 (brs, 1H), 8.92 (dd, J = 4.0, 1.2 Hz, 1H), 8.56 (d, J = 8.7 Hz, 1H), 8.02 (d, J = 8.3 Hz, 1H), 7.51 (dd, J = 8.7, 4.1 Hz, 1H), 6.96 (d, J = 8.4 Hz, 1H), 3.83 (d, J = 10.0 Hz, 1H), 3.79 (d, J = 10.2 Hz, 1H), 3.75 (d, J = 10.1 Hz, 1H), 3.58 (dd, J = 10.1, 3.7 Hz, 1H), 2.18 − 2.11 (m, 1H), 1.44 (dd, J = 8.0, 4.3 Hz, 1H), 1.20 ppm (t, J = 4.7 Hz, 1H). ^{13}**C NMR** (100 MHz, DMSO-d_6) δ = 173.31, 151.64, 150.93, 148.70, 136.37, 134.13, 120.69, 120.53, 118.46, 111.22, 101.60, 53.09, 53.05, 28.81, 25.94, 16.35 ppm. **HRMS** (ESI) m/z: [M + H]$^+$ calcd for C$_{16}$H$_{14}$N$_3$O$_2$ 280.1081; found: 280.1082.

(1S)-3-(8-Cyanoquinolin-5-yl)-3-azabicyclo[3.1.0]hexane-1-car-boxamide 6. To a solution of **5** (80 mg, 0.29 mmol) in *N,N*-dimethylformamide (2 mL) was added 2-(7-azabenzotriazol-1-yl)-*N,N,N′,N′*-tetramethyluronium hexafluorophosphate (166.3 mg, 0.44 mmol) and *N,N*-diisopropylethylamine (56.9 mg, 0.44 mmol), the mixture was stirred at room temperature for 10 min. Ammonium bicarbonate (45.9 mg, 0.58 mmol) was added, and the mixture was stirred at room temperature for 5.5 h, and then quenched by saturated aqueous ammonium chloride and extracted with ethyl acetate. The organic layers were combined, washed with brine, dried by anhydrous sodium sulfate, filtered and concentrated under reduced pressure. The crude product was purified by flash column chromatography ($V_{\text{Dichloromethane}}/V_{\text{Methanol}}$ = 15:1) to afford product **6** (52 mg, 65% yield, yellow solid). ^{1}**H NMR** (400 MHz, DMSO-d_6) δ = 8.96 (dd, J = 4.1, 1.4 Hz, 1H), 8.66 (dd, J = 8.7, 1.4 Hz, 1H), 8.08 (d, J = 8.3 Hz, 1H), 7.54 (dd, J = 8.7, 4.1 Hz, 1H), 7.24 (s, 1H), 7.09 (s, 1H), 6.98 (d, J = 8.4 Hz, 1H), 3.90 (d, J = 10.1 Hz, 1H), 3.83 (d, J = 10.1 Hz, 1H), 3.78 (d, J = 10.1 Hz, 1H), 3.60 (dd, J = 10.0, 3.7 Hz, 1H), 2.12−2.02 (m, 1H), 1.35 (dd, J = 8.0, 4.3 Hz, 1H), 1.08 ppm (t, J = 4.6 Hz, 1H). ^{13}**C NMR** (100 MHz, DMSO-d_6) δ = 172.66, 151.65, 151.04, 148.82, 136.44, 134.35, 120.54, 120.42, 118.51, 110.90, 101.17, 53.86, 53.13, 30.40, 24.51, 15.89 ppm. **HRMS** (ESI) m/z: [M + H]$^+$ calcd for C$_{16}$H$_{15}$N$_4$O 279.1240; found: 279.1242.

(1S)-3-(8-Cyanoquinolin-5-yl)-N-(1-methylpiperidin-4-yl)-3-aza-bicyclo [3.1.0] hexane-1-carboxamide 7. The title compound **7** was prepared from **5** (80 mg, 0.29 mmol) and 1-methylpiperidin-4-amine (33 mg, 0.29 mol) through the similar **Procedure** for the Synthesis of **6**, and purified by flash column chromatography ($V_{\text{Dichloromethane}}/V_{\text{Methanol}}$ = 40:1) (90 mg, 83% yield, white solid). ^{1}**H NMR** (400 MHz, DMSO-d_6) δ = 8.96 (d, J = 3.9 Hz, 1H), 8.64 (d, J = 8.6 Hz, 1H), 8.09 (d, J = 8.3 Hz, 1H), 7.55 (dd, J = 8.7, 4.1 Hz, 1H), 7.44 (d, J = 7.7 Hz, 1H), 7.00 (d, J = 8.4 Hz, 1H), 3.93 (d, J = 10.0 Hz, 1H), 3.77 (d, J = 11.1 Hz, 2H), 3.62−3.52 (m, 2H), 2.74 (d, J = 11.0 Hz, 2H), 2.14 (s, 3H), 2.10− 2.04 (m, 1H), 1.90 (t, J = 11.5 Hz, 2H), 1.71−1.61 (m, 2H), 1.54−1.41 (m, 2H), 1.32 (dd, J = 8.0, 4.2 Hz, 1H), 1.10 ppm (t, J = 4.5 Hz, 1H). ^{13}**C NMR** (100 MHz, DMSO-d_6) δ = 169.57, 151.65, 151.06, 148.74, 136.42, 134.27, 120.65, 120.51, 118.46, 111.15, 101.44, 54.46, 53.81, 52.93, 46.25, 45.79, 31.36, 30.52, 24.35, 15.81 ppm. **HRMS** (ESI) m/z: [M + H]$^+$ calcd for C$_{22}$H$_{26}$N$_5$O 376.2132; found: 376.2134.

Methyl (1S,5R)-3-(8-Cyanoquinolin-5-yl)-5-(trifluoromethyl)-3-azabicyclo [3.1.0] hexane-1-carboxylate 48. To an oven-dried 500 mL round-bottom flask equipped with a stirring bar was added **41** (25.0 g, 0.12 mol), 5-bromoquinoline-8-carbonitrile (30.2 g, 0.13 mol), cesium carbonate (156 g, 0.48 mol), and dry 1,4-dioxane (250 mL). The resultant mixture was degassed three times, and then Ruphos Pd G3 (5.0 g, 6 mmol) was added to the above reaction mixture under argon atmosphere. The reaction mixture was heated in an oil bath at 80 °C for 3 h. The resulting solution was filtered. The solvent was extracted with ethyl acetate, washed with brine, dried by anhydrous sodium sulfate, filtered and concentrated under reduced pressure. The crude product was purified by flash column chromatography ($V_{\text{Petroleum ether}}/V_{\text{Ethyl acetate}}$ = 5:1) to afford product **48** (39.4 g, 91% yield, yellow solid). ^{1}**H NMR** (400 MHz, CDCl$_3$) δ = 8.94 (dd, J = 4.2, 1.6 Hz, 1H), 8.29 (dd, J = 8.6, 1.6 Hz, 1H), 7.89 (d, J = 8.0 Hz, 1H), 7.44 (dd, J = 8.6, 4.2 Hz, 1H), 7.02 (d, J = 8.1 Hz, 1H), 3.92 (d, J = 10.1 Hz, 1H), 3.82 (d, J = 9.8 Hz, 1H), 3.80−3.75 (m, 1H), 3.73 (s, 3H), 3.61 (d, J = 9.8 Hz, 1H), 2.18 (d, J = 5.6 Hz, 1H), 1.94−1.87 ppm (m, 1H). ^{13}**C NMR** (100 MHz, CDCl$_3$) δ = 167.69, 151.81, 149.20, 148.56, 135.59, 132.52, 124.27 (q, J = 271 Hz, 1C), 122.37, 121.11, 117.52, 113.15, 106.54, 54.19, 52.50, 52.35, 37.43 (q, J = 36 Hz, 1C), 33.44, 15.69 ppm. ^{19}**F NMR** (377 MHz, CDCl$_3$) δ = −63.73 ppm. **HRMS** (ESI) m/z: [M + H]$^+$ calcd for C$_{18}$H$_{15}$F$_3$N$_3$O$_2$ 362.1111; found: 362.1113.

(1S,5R)-3-(8-Cyanoquinolin-5-yl)-5-(trifluoromethyl)-3-azabicyclo[3.1.0]hexane-1-carboxylic Acid 49. To a solution of **48** (10 g, 0.028 mol) in THF/H$_2$O = 4/1(100 mL) was added lithium hydroxide (4.7 g, 0.112 mol). The resulting mixture was stirred vigorously at room temperature for 10 h. 2 N HCl aq was added, and the pH was adjusted to 3−4, and extracted with ethyl acetate. The

organic layers were combined, washed with brine, dried by anhydrous sodium sulfate, filtered, and concentrated under reduced pressure. The crude product was purified by flash column chromatography ($V_{\text{Petroleum ether}}/V_{\text{Ethyl acetate}}$ = 1:1) to afford the product **49** (8.2 g, 84% yield, white solid). **¹H NMR** (400 MHz, CDCl₃) δ = 9.08 (dd, J = 4.1, 1.4 Hz, 1H), 8.35 (dd, J = 8.6, 1.4 Hz, 1H), 8.02 (d, J = 8.0 Hz, 1H), 7.53 (dd, J = 8.6, 4.2 Hz, 1H), 7.11 (d, J = 8.1 Hz, 1H), 3.99 (d, J = 10.1 Hz, 1H), 3.89 (d, J = 9.9 Hz, 1H), 3.84 (d, J = 10.1 Hz, 1H), 3.69 (d, J = 9.9 Hz, 1H), 2.31 (d, J = 5.4 Hz, 1H), 2.01 ppm (d, J = 4.1 Hz, 1H). **¹³C NMR** (100 MHz, CDCl₃) δ = 172.55, 152.15, 149.27, 148.71, 135.97, 132.76, 124.34 (q, J = 272 Hz, 1C), 122.77, 121.41, 117.48, 113.53, 107.12, 54.29, 52.70, 38.60 (q, J = 36.0 Hz, 1C), 33.49, 16.44 ppm. **¹⁹F NMR** (377 MHz, CDCl₃) δ = −63.43 ppm. **HRMS** (ESI) m/z: $[M + H]^+$ calcd for $C_{17}H_{13}F_3N_3O_2$ 348.0954; found: 348.0957.

*(1S,5R)-3-(8-Cyanoquinolin-5-yl)-5-(trifluoromethyl)-3-azabicyclo[3.1.0]hexane-1-carboxamide **8***. The title compound **8** was prepared from **49** (100 mg, 0.29 mmol) and ammonium bicarbonate (45.9 mg, 0.58 mol) through the similar *Procedure* for the Synthesis of **6**, and purified by flash column chromatography ($V_{\text{Dichloromethane}}/V_{\text{Methanol}}$ = 10:1)(52 mg, 52% yield, yellow solid). **¹H NMR** (400 MHz, CD₃OD) δ = 8.95 (dd, J = 4.2, 1.4 Hz, 1H), 8.59 (dd, J = 8.7, 1.4 Hz, 1H), 8.09 (d, J = 8.1 Hz, 1H), 7.60 (dd, J = 8.6, 4.2 Hz, 1H), 7.25 (d, J = 8.2 Hz, 1H), 3.96 (s, 2H), 3.93 (d, J = 9.7 Hz, 1H), 3.81 (d, J = 9.7 Hz, 1H), 2.02 (d, J = 6.0 Hz, 1H), 1.81 ppm (d, J = 5.8 Hz, 1H). **¹³C NMR** (100 MHz, DMSO-d_6) δ = 167.21, 151.97, 150.24, 148.39, 136.42, 133.97, 125.24 (q, J = 272 Hz, 1C). 121.38, 121.25, 118.11, 112.71, 103.47, 55.41, 52.01, 35.75, 34.79 (q, J = 34.7 Hz, 1C), 13.96 ppm. **¹⁹F NMR** (377 MHz, CD₃OD) δ = −66.37 ppm. **HRMS** (ESI) m/z: $[M + H]^+$ calcd for $C_{17}H_{14}F_3N_4O$ 347.1114; found: 347.1115.

*(1S,5R)-3-(8-Cyanoquinolin-5-yl)-N-(piperidin-4-yl)-5-(trifluoromethyl)-3-azabicyclo[3.1.0]hexane-1-carboxamide **9***. The title compound **9** was prepared from **49** (100 mg, 0.29 mol) and *tert*-butyl 4-aminopiperazine-1-carboxylate (69.2 mg, 0.34 mol) through the similar *Procedure* for the Synthesis of **6**, and purified by flash column chromatography ($V_{\text{Dichloromethane}}/V_{\text{Methanol}}$ = 10:1)(32 mg, 27% yield, yellow solid). **¹H NMR** (400 MHz, CDCl₃) δ = 9.01 (d, J = 3.5 Hz, 1H), 8.32 (d, J = 8.5 Hz, 1H), 7.95 (d, J = 7.9 Hz, 1H), 7.47 (dd, J = 8.3, 3.9 Hz, 1H), 7.03 (d, J = 7.8 Hz, 1H), 4.44 (d, J = 12.2 Hz, 1H), 4.18−4.02 (m, 1H), 3.89 (d, J = 9.6 Hz, 1H), 3.84−3.72 (m, 3H), 3.22 (dt, J = 23.9, 11.5 Hz, 1H), 2.98 (s, 1H), 2.90 − 2.72 (m, 1H), 1.99−1.78 (m, 3H), 1.72 (d, J = 5.3 Hz, 1H), 1.49 (s, 2H), 1.40−1.15 ppm (s, 2H).**¹³C NMR** (100 MHz, CDCl₃) δ = 164.57, 152.01, 149.39, 148.87, 135.74, 132.59, 124.67 (q, J = 271 Hz, 1C), 122.51, 121.18, 117.64, 113.14, 106.74, 55.78 (d, J = 20 Hz, 1C), 52.32, 48.26 (d, J = 34 Hz, 1C), 45.03, 41.16 (d, J = 18 Hz, 1C), 36.1−34.7 (m, 2C), 14.94 ppm (d, J = 14 Hz, 1C). **¹⁹F NMR** (377 MHz, CDCl₃) δ = −65.53 ppm. **HRMS** (ESI) m/z: $[M + H]^+$ calcd for $C_{22}H_{23}F_3N_5O$ 430.1849; found: 430.1855.

*(1S,5R)-3-(8-Cyanoquinolin-5-yl)-N-(1-methylpiperidin-4-yl)-5-(trifluoromethyl)-3-azabicyclo[3.1.0]hexane-1-carboxamide **10***. The title compound **10** was prepared from **49** (40.0 mg, 0.12 mol) and 1-methylpiperidin-4-amine (26.3 mg, 0.24 mol) through the similar *Procedure* for the Synthesis of **6**, and purified by flash column chromatography ($V_{\text{Dichloromethane}}/V_{\text{Methanol}}$ = 5:1)(30 mg, 56% yield, yellow solid). **¹H NMR** (400 MHz, CDCl₃) δ = 8.97 (dd, J = 4.2, 1.5 Hz, 1H), 8.32 (dd, J = 8.6, 1.6 Hz, 1H), 7.88 (d, J = 8.1 Hz, 1H), 7.45 (dd, J = 8.6, 4.2 Hz, 1H), 7.04 (d, J = 8.1 Hz, 1H), 5.94 (d, J = 8.0 Hz, 1H), 4.02 (d, J = 9.9 Hz, 1H), 3.92−3.77 (m, 4H), 2.79 (d, J = 9.0 Hz, 2H), 2.27 (s, 3H), 2.08 (t, J = 11.5 Hz, 2H), 1.99−1.88 (m, 3H), 1.79II (d, J = 5.8 Hz, 1H), 1.59−1.44 ppm (m, 2H). **¹³C NMR** (100 MHz, DMSO-d_6) δ = 164.97, 151.94, 149.55, 148.83, 135.72, 132.71, 124.67 (q, J = 272 Hz, 1C), 122.42, 121.13, 117.80, 113.10, 106.41, 56.11, 54.34, 52.25, 46.72, 46.10, 36.20, 35.28 (q, J = 36 Hz, 1C), 31.82, 31.77, 13.95 ppm. **¹⁹F NMR** (377 MHz, CDCl₃) δ = −64.85 ppm. **HRMS** (ESI) m/z: $[M + H]^+$ calcd for $C_{23}H_{25}F_3N_5O$ 444.2006; found: 444.2010.

(1S,5R)-3-(8-Cyanoquinolin-5-yl)-N-(1-(2-hydroxyethyl)piperidin-4-yl)-5-(trifluoromethyl)-3-azabicyclo[3.1.0]hexane-1-carboxamide

11. The title compound **11** was prepared from **49** (55 mg, 0.16 mol) and 4-amino-1-piperidine-ethanol (46.1 mg, 0.32 mol) through the similar *Procedure* for the Synthesis of **6**, and purified by flash column chromatography ($V_{\text{Dichloromethane}}/V_{\text{Methanol}}$ = 1:1)(55 mg, 83% yield, yellow solid). **¹H NMR** (400 MHz, DMSO-d_6) δ = 9.00 (d, J = 3.1 Hz, 1H), 8.63 (d, J = 7.9 Hz, 1H), 8.16 (d, J = 8.2 Hz, 1H), 8.02 (d, J = 7.7 Hz, 1H), 7.60 (dd, J = 8.6, 4.1 Hz, 1H), 7.22 (d, J = 8.3 Hz, 1H), 4.35 (s, 1H), 4.01 (d, J = 9.9 Hz, 1H), 3.97−3.89 (m, 2H), 3.82 (d, J = 9.8 Hz, 1H), 3.64−3.52 (m, 1H), 3.46 (dd, J = 11.1, 5.6 Hz, 2H), 2.82 (d, J = 8.3 Hz, 2H), 2.35 (t, J = 6.3 Hz, 2H), 2.03−1.92 (m, 3H), 1.70−1.57 (m, 3H), 1.50−1.34 ppm (m, 2H).**¹³C NMR** (100 MHz, DMSO-d_6) δ = 164.40, 151.91, 150.21, 148.39, 136.35, 133.94, 125.20 (q, J = 271 Hz, 1C), 121.32, 121.20, 118.12, 112.67, 103.43, 60.23, 58.72, 55.55, 52.65, 51.91, 46.90, 36.14, 34.37 (q, J = 34 Hz, 1C), 31.18 (d, J = 4.9 Hz, 1C), 13.79 ppm. **¹⁹F NMR** (377 MHz, CDCl₃) δ = −63.63 ppm. **HRMS** (ESI) m/z: $[M + H]^+$ calcd for $C_{24}H_{27}F_3N_5O_2$ 474.2116; found: 474.2116.

*(1S,5R)-3-(8-Cyanoquinolin-5-yl)-N-(pyridin-4-yl)-5-(trifluoromethyl)-3-azabicyclo[3.1.0]hexane-1-carboxamide **12***. The title compound **12** was prepared from **49** (200 mg, 0.57 mol) and pyridin-4-amine (54 mg, 0.51 mol) through the similar *Procedure* for the Synthesis of **6**, and purified by flash column chromatography ($V_{\text{Dichloromethane}}/V_{\text{Methanol}}$ = 20:1)(253 mg, 83% yield, yellow solid). **¹H NMR** (400 MHz, CDCl₃) δ = 9.65 (s, 1H), 8.79 (dd, J = 4.1, 1.3 Hz, 1H), 8.41 (d, J = 5.6 Hz, 2H), 8.29 (dd, J = 8.6, 1.3 Hz, 1H), 7.66 (d, J = 8.1 Hz, 1H), 7.63 (d, J = 6.3 Hz, 2H), 7.37 (dd, J = 8.6, 4.2 Hz, 1H), 6.90 (d, J = 8.2 Hz, 1H), 4.23 (d, J = 9.9 Hz, 1H), 4.05 (d, J = 9.8 Hz, 1H), 3.95 (d, J = 9.8 Hz, 1H), 3.87 (d, J = 9.8 Hz, 1H), 2.16 (d, J = 6.0 Hz, 1H), 1.80 ppm (d, J = 5.9 Hz, 1H). **¹³C NMR** (100 MHz, CDCl₃) δ = 165.20, 151.71, 150.08, 149.82, 148.62, 145.53, 135.69, 132.97, 124.55 (q, J = 271 Hz, 1C), 121.87, 121.06, 118.32, 114.18, 112.55, 104.84, 56.13, 52.23, 37.40, 36.10 (q, J = 36 Hz, 1C), 14.74 ppm. **¹⁹F NMR** (377 MHz, CDCl₃) δ = −65.06 ppm. **HRMS** (ESI) m/z: $[M + H]^+$ calcd for $C_{22}H_{17}F_3N_5O$ 424.1380; found: 424.1381.

*(1S,5R)-3-(8-Cyanoquinolin-5-yl)-N-(6-morpholinopyridin-3-yl)-5-(trifluoromethyl)-3-azabicyclo[3.1.0]hexane-1-carboxamide **13***. The title compound **13** was prepared from **49** (50 mg, 0.14 mol) and 6-morpholinopyridin-3-amine (25.1 mg, 0.14 mol) through the similar *Procedure* for the Synthesis of **6**, and purified by flash column chromatography ($V_{\text{Dichloromethane}}/V_{\text{Methanol}}$ = 15:1)(47 mg, 92%, yellow solid). **¹H NMR** (400 MHz, DMSO-d_6) δ = 9.98 (s, 1H), 9.01 (dd, J = 4.1, 1.2 Hz, 1H), 8.66 (dd, J = 8.6, 1.1 Hz, 1H), 8.30 (d, J = 2.5 Hz, 1H), 8.18 (d, J = 8.2 Hz, 1H), 7.76 (dd, J = 9.1, 2.6 Hz, 1H), 7.61 (dd, J = 8.7, 4.2 Hz, 1H), 7.26 (d, J = 8.3 Hz, 1H), 6.84 (d, J = 9.1 Hz, 1H), 4.14−4.06 (m, 2H), 4.00 (d, J = 9.9 Hz, 1H), 3.89 (d, J = 9.9 Hz, 1H), 3.72−3.66 (m, 4H), 3.40−3.35 (m, 4H), 2.10 (d, J = 6.0 Hz, 1H), 1.76 ppm (d, J = 5.9 Hz, 1H). **¹³C NMR** (100 MHz, DMSO-d_6) δ = 164.04, 156.26, 151.93, 150.12, 148.39, 140.00, 136.36, 133.92, 130.87, 126.39, 125.16 (q, J = 271 Hz, 1C), 121.34, 121.21, 118.10, 112.69, 106.71, 103.53, 65.90, 55.58, 51.90, 45.49, 36.83, 34.79 (q, J = 34 Hz, 1C), 14.13 ppm. **¹⁹F NMR** (377 MHz, DMSO-d_6) δ = −63.76 ppm. **HRMS** (ESI) m/z: $[M + H]^+$ calcd for $C_{26}H_{24}F_3N_6O_2$ 509.1907; found: 509.1914.

*(1S,5R)-3-(8-Cyanoquinolin-5-yl)-N-(4-morpholinophenyl)-5-(trifluoromethyl)-3-azabicyclo[3.1.0]hexane-1-carboxamide **14***. The title compound **14** was prepared from **49** (50 mg, 0.14 mol) and 4-morpholinoaniline (28.5 mg, 0.16 mol) through the similar *Procedure* for the Synthesis of **6**, and purified by flash column chromatography ($V_{\text{Dichloromethane}}/V_{\text{Methanol}}$ = 15:1)(36 mg, 87%, yellow solid). **¹H NMR** (400 MHz, DMSO-d_6) δ = 9.88 (s, 1H), 9.01 (dd, J = 4.1, 1.4 Hz, 1H), 8.67 (dd, J = 8.7, 1.4 Hz, 1H), 8.18 (d, J = 8.2 Hz, 1H), 7.61 (dd, J = 8.7, 4.2 Hz, 1H), 7.45 (d, J = 9.0 Hz, 2H), 7.26 (d, J = 8.3 Hz, 1H), 6.91 (d, J = 9.1 Hz, 2H), 4.12 (d, J = 10.0 Hz, 1H), 4.08 (d, J = 10.1 Hz, 1H), 3.99 (d, J = 9.8 Hz, 1H), 3.90 (d, J = 9.8 Hz, 1H), 3.76−3.69 (m, 4H), 3.07−3.01 (m, 4H), 2.08 (d, J = 4.5 Hz, 1H), 1.72 ppm (d, J = 5.9 Hz, 1H). **¹³C NMR** (100 MHz, DMSO-d_6) δ = 163.52, 151.93, 150.18, 148.42, 147.73, 136.36, 133.95, 130.69, 125.21 (q, J = 271 Hz, 1C), 121.31, 121.26, 121.19, 118.12, 115.22, 112.64, 103.42, 66.06, 55.67, 51.93, 48.79, 37.11, 34.63 (q, J = 35 Hz,

1C), 14.15 ppm. ^{19}F NMR (377 MHz, DMSO-d_6) δ = −63.80 ppm. HRMS (ESI) m/z: [M + H]$^+$ calcd for $C_{27}H_{25}F_3N_5O_2$ 508.1955; found: 508.1960.

(1S,5R)-3-(8-Cyanoquinolin-5-yl)-N-(1-(pyridin-2-yl)piperidin-4-yl)-5-(trifluoromethyl)-3-azabicyclo[3.1.0]hexane-1-carboxamide **15**. The title compound **15** was prepared from **49** (150 mg, 0.43 mol) and 1-(pyridin-2-yl)piperidin-4-amine (84 mg, 0.47 mol) through the similar *Procedure* for the Synthesis of **6**, and purified by flash column chromatography ($V_{Dichloromethane}/V_{Methanol}$ = 15:1)(141 mg, 85% yield, yellow solid). ^{1}**H NMR** (400 MHz, CDCl$_3$) δ = 8.99 (dd, J = 4.1, 1.3 Hz, 1H), 8.32 (dd, J = 8.6, 1.3 Hz, 1H), 8.20−8.13 (m, 1H), 7.90 (d, J = 8.1 Hz, 1H), 7.50−7.44 (m, 2H), 7.04 (d, J = 8.1 Hz, 1H), 6.67 (d, J = 8.6 Hz, 1H), 6.61 (dd, J = 7.0, 5.1 Hz, 1H), 5.97 (d, J = 7.9 Hz, 1H), 4.30−4.19 (m, 2H), 4.16−4.05 (m, 1H), 4.02 (d, J = 9.8 Hz, 1H), 3.90−3.76 (m, 2H), 3.00 (t, J = 11.6 Hz, 2H), 2.03 (dd, J = 9.4, 3.4 Hz, 2H), 1.89 (d, J = 5.9 Hz, 1H), 1.80 (d, J = 5.8 Hz, 1H), 1.57−1.41 ppm (m, 2H). ^{13}**C NMR** (100 MHz, CDCl$_3$) δ = 165.00, 158.88, 152.01, 149.52, 148.88, 147.69, 137.71, 135.75, 132.68, 122.49, 121.83 (q, J = 271 Hz, 1C), 121.18, 117.79, 113.17, 113.12, 107.34, 106.60, 56.11, 52.30, 47.59, 44.38, 36.19, 35.40 (q, J = 36 Hz, 1C), 31.23 (d, J = 3.8 Hz, 1C) 13.95 ppm. ^{19}**F NMR** (377 MHz, CDCl$_3$) δ = −64.80 ppm. **HRMS** (ESI) m/z: [M + H]$^+$ calcd for $C_{27}H_{26}F_3N_6O$ 507.2115; found: 507.2123.

(1S,5R)-3-(8-Cyanoquinolin-5-yl)-N-(((S)-4-methylmorpholin-2-yl)methyl)-5-(trifluoromethyl)-3-azabicyclo[3.1.0]hexane-1-carbox-amide **16**. The title compound **16** was prepared from **49** (50 mg, 0.14 mol) and (S)-(4-methylmorpholin-2-yl)methanamine (23 mg, 0.17 mmol) through the similar *Procedure* for the Synthesis of **6**, and purified by flash column chromatography ($V_{Dichloromethane}/V_{Methanol}$ = 15:1)(24 mg, 37%, yellow solid). ^{1}**H NMR** (400 MHz, CDCl$_3$) δ = 8.96 (dd, J = 4.2, 1.5 Hz, 1H), 8.30 (dd, J = 8.6, 1.5 Hz, 1H), 7.89 (d, J = 8.1 Hz, 1H), 7.44 (dd, J = 8.6, 4.2 Hz, 1H), 7.03 (d, J = 8.1 Hz, 1H), 6.41 (t, J = 5.2 Hz, 1H), 3.97 (d, J = 9.8 Hz, 1H), 3.88−3.79 (m, 3H), 3.75 (d, J = 9.7 Hz, 1H), 3.67−3.53 (m, 3H), 3.22−3.13 (m, 1H), 2.67 (d, J = 11.2 Hz, 1H), 2.60 (d, J = 11.4 Hz, 1H), 2.24 (s, 3H), 2.06 (td, J = 11.4, 3.3 Hz, 1H), 1.88 (d, J = 5.9 Hz, 1H), 1.84 −1.76 ppm (m, 2H). ^{13}**C NMR** (100 MHz, CDCl$_3$) δ = 165.60, 151.92, 149.47, 148.79, 135.69, 132.67, 124.59 (q, J = 271 Hz, 1C), 122.43, 121.11, 117.71, 113.11, 106.46, 73.88, 66.52, 57.35, 55.94, 54.55, 52.26, 46.12, 42.19, 36.03, 35.27 (q, J = 35 Hz, 1C), 13.83 ppm. ^{19}**F NMR** (377 MHz, CDCl$_3$) δ = −64.87 ppm. **HRMS** (ESI) m/z: [M + H]$^+$ calcd for $C_{23}H_{25}F_3N_5O_2$ 460.1955; found: 460.1957.

General Procedure for the Synthesis of Compounds 17−21.
5-((1S,5R)-1-(5-Amino-1,3,4-oxadiazol-2-yl)-5-(trifluoromethyl)-3-azabicyclo[3.1.0]hexan-3-yl)quinoline-8-carbonitrile **17**. To a solution of **49** (100 mg, 0.29 mmol) in phosphorus oxychloride (10 mL) was added semicarbazide hydrochloride (48.3 mg, 0.44 mmol), the mixture was stirred at room temperature for 1h, then quenched by saturated aqueous sodium bicarbonate, the pH was adjusted to 9 and extracted with ethyl acetate. The organic layers were combined, washed with brine, dried by anhydrous sodium sulfate, filtered and concentrated under reduced pressure. The crude product was purified by flash column chromatography ($V_{Dichloromethane}/V_{Methanol}$ = 15:1) to afford the product **17** (80 mg, 71% yield, yellow solid). ^{1}**H NMR** (400 MHz, DMSO-d_6) δ = 9.05−8.99 (m, 1H), 8.68 (dd, J = 8.6, 1.2 Hz, 1H), 8.18 (d, J = 8.2 Hz, 1H), 7.62 (dd, J = 8.6, 4.2 Hz, 1H), 7.29 (d, J = 8.3 Hz, 1H), 7.16 (s, 2H), 4.15 (d, J = 10.2 Hz, 1H), 4.06 (d, J = 10.0 Hz, 1H), 3.92 (d, J = 5.0 Hz, 1H), 3.89 (d, J = 4.9 Hz, 1H), 2.11−2.03 ppm (m, 2H). ^{13}**C NMR** (100 MHz, DMSO-d_6) δ = 164.23, 154.10, 151.98, 149.73, 148.28, 136.36, 133.86, 124.86 (q, J = 272 Hz, 1C), 121.58, 121.38, 117.99, 113.14, 104.11, 54.88, 51.56, 34.44 (q, J = 35 Hz, 1C). 27.23, 14.38 ppm. ^{19}**F NMR** (377 MHz, DMSO-d_6) δ = −64.08 ppm. **HRMS** (ESI) m/z: [M + H]$^+$ calcd for $C_{18}H_{14}F_3N_6O$ 387.1176; found: 387.1177.

(1S,5R)-3-(8-Cyanoquinolin-5-yl)-5-(trifluoromethyl)-3-azabicyclo[3.1.0]hexane-1-carbohydrazide **50**. To a solution of **48** (27 g, 0.075 mol) in 54 mL methanol was added hydrazine hydrate (54 mL). Then the mixture was stirring for 3h at 85 °C. TLC showed no materials was remained. The reaction mixture was concentrated and dissolved by acetonitrile, the mixture was filtered to afford the

product **50** (21 g, 79% yield, yellow solid). ^{1}**H NMR** (400 MHz, DMSO-d_6) δ = 9.49 (s, 1H), 9.00 (dd, J = 4.1, 1.5 Hz, 1H), 8.62 (dd, J = 8.7, 1.5 Hz, 1H), 8.16 (d, J = 8.2 Hz, 1H), 7.60 (dd, J = 8.7, 4.2 Hz, 1H), 7.22 (d, J = 8.3 Hz, 1H), 4.42 (brs, 2H), 4.00−3.88 (m, 3H), 3.79 (d, J = 9.8 Hz, 1H), 1.98 (d, J = 6.0 Hz, 1H), 1.63 ppm (d, J = 5.8 Hz, 1H). ^{13}**C NMR** (100 MHz, DMSO-d_6) δ = 164.65, 151.97, 150.20, 148.38, 136.41, 133.94, 125.13 (q, J = 271 Hz, 1C), 121.40, 121.24, 118.08, 112.73, 103.50, 55.31, 51.91, 34.61, 34.03 (q, J = 35 Hz, 1C), 13.50 ppm. ^{19}**F NMR** (377 MHz, DMSO-d_6) δ = −63.56 ppm. **HRMS** (ESI) m/z: [M + H]$^+$ calcd for $C_{17}H_{15}F_3N_5O$ 362.1223; found: 362.1224.

Synthesis of Compound 18. *tert-Butyl (S)-2-(5-((1S,5R)-3-(8-cyanoquinolin-5-yl)-5-(trifluoromethyl)-3-azabicyclo[3.1.0]hexan-1-yl)-1,3,4-oxadiazol-2-yl)morpholine-4-carboxylate.* To a solution of (S)-4-(tert-butoxycarbonyl)morpholine-2-carboxylic acid (32 mg, 0.13 mmol) in N,N-dimethylformamide was added 2-(7-azabenzo-triazol-1-yl)-N,N,N′,N′-tetramethyluronium hexafluorophosphate (59 mg, 0.15 mmol), N,N-diisopropylethylamine (50 mg, 0.39 mmol), and the mixture was stirred for 5 min. The reaction mixture was then added to (1S, 5R)-3-(8-cyanoquinolin-5-yl)-5-(trifluoromethyl)-3-azabicyclo-[3.1.0]hexane-1-carbohydrazide **50** (50 mg, 0.13 mmol) and stirred for 0.5 h. TLC showed that no starting material remained. After adding Burgess reagent (92.8 mg, 0.39 mmol), the mixture was stirred for 5 h at 20 °C. The solution was concentrated under reduced pressure and purified by flash column chromatography ($V_{Dichloromethane}/V_{Methanol}$ = 10:1) to afford the product (40 mg, 41% yield, yellow solid).

5-((1S,5R)-1-(5-((S)-morpholin-2-yl)-1,3,4-oxadiazol-2-yl)-5-(tri-fluoromethyl)-3-azabicyclo[3.1.0]hexan-3-yl)quinoline-8-carboni-trile. To a solution of above-obtained compound (40 mg, 0.072 mmol) in dioxane was added 2N HCl in dioxane (3 mL), and the mixture was stirring for 2 h at 20 °C. TLC showed that no starting material remained. The reaction mixture was concentrated under vacuum to afford the product (50 mg, 100% yield) as yellow solid. This crude mixture was used directly in the next step without further purification.

5-((1S,5R)-1-(5-((S)-4-Methylmorpholin-2-yl)-1,3,4-oxadiazol-2-yl)-5-(trifluoromethyl)-3-azabicyclo[3.1.0]hexan-3-yl)quinoline-8-carbonitrile **18**. To a solution of above-obtained compound in methanol (2 mL) was added triethylamine (0.02 mL), paraformalde-hyde (64 mg, 0.72 mmol), and sodium cyanoborohydride (27 mg, 0.72 mmol). The reaction mixture was heated in an oil bath at 80 °C for 3 h. The crude product was concentrated under reduced pressure and purified by flash column chromatography ($V_{Dichloromethane}/V_{Methanol}$ = 5:1) to afford product **18** (22 mg, 65% yield for two steps, yellow solid). ^{1}**H NMR** (400 MHz, CDCl$_3$) δ = 9.09 (dd, J = 4.1, 1.5 Hz, 1H), 8.36 (dd, J = 8.6, 1.5 Hz, 1H), 8.05 (d, J = 8.0 Hz, 1H), 7.53 (dd, J = 8.6, 4.2 Hz, 1H), 7.17 (d, J = 8.1 Hz, 1H), 4.89 (dd, J = 9.6, 2.5 Hz, 1H), 4.15 (d, J = 9.9 Hz, 1H), 4.06−3.93 (m, 3H), 3.90−3.78 (m, 2H), 3.07 (d, J = 11.4 Hz, 1H), 2.71 (d, J = 11.7 Hz, 1H), 2.57−2.50 (m, 1H), 2.42−2.31 (m, 5H), 2.24 ppm (d, J = 5.8 Hz, 1H). ^{13}**C NMR** (100 MHz, CDCl$_3$) δ = 164.80, 162.40, 152.21, 148.83, 148.80, 135.75, 132.43, 124.16 (q, J = 272 Hz, 1C), 122.77, 121.50, 117.46, 113.76, 107.69, 69.18, 66.86, 56.60, 55.03, 54.15, 52.28, 46.06, 36.24 (q, J = 35 Hz, 1C), 27.00, 14.90 ppm. ^{19}**F NMR** (377 MHz, CDCl$_3$) δ = −65.32 ppm. **HRMS** (ESI) m/z: [M + H]$^+$ calcd for $C_{23}H_{22}F_3N_6O_2$ 471.1751; found: 471.1755.

5-((1S,5R)-1-(5-(1-Methylpiperidin-4-yl)-1,3,4-oxadiazol-2-yl)-5-(trifluoromethyl)-3-azabicyclo[3.1.0]hexan-3-yl)quinoline-8-car-bonitrile **19**. The title compound **19** was prepared from **50** (5.0 g, 13.9 mmol) and 1-methylpiperidine-4-carboxylic acid (1.99 g, 13.9 mmol) through the similar *Procedure* for the Synthesis of **18**, and purified by flash column chromatography ($V_{Dichloromethane}/V_{Methanol}$ = 5:1) (3.2 g, 49% yield for two steps, white solid). ^{1}**H NMR** (400 MHz, CDCl$_3$) δ = 9.00 (dd, J = 4.2, 1.5 Hz, 1H), 8.34 (dd, J = 8.6, 1.5 Hz, 1H), 7.97 (d, J = 8.0 Hz, 1H), 7.48 (dd, J = 8.6, 4.2 Hz, 1H), 7.12 (d, J = 8.1 Hz, 1H), 4.08 (d, J = 9.9 Hz, 1H), 3.96 (d, J = 10.0 Hz, 1H), 3.92 (d, J = 9.8 Hz, 1H), 3.76 (d, J = 9.8 Hz, 1H), 2.93 − 2.80 (m, 3H), 2.31 − 2.24 (m, 4H), 2.19 (d, J = 5.8 Hz, 1H), 2.15−2.00 (m, 4H), 1.97−1.85 ppm (m, 2H).^{13}**C NMR** (100 MHz, CDCl$_3$) δ = 169.58, 161.67, 152.07, 148.86, 148.72, 135.71, 132.46, 124.17 (q, J =

271 Hz, 1C), 122.65, 121.39, 117.46, 113.62, 107.33, 54.91, 54.40, 52.21, 46.15, 36.07 (q, J = 36 Hz, 1C), 32.54,, 28.91 (d, J = 6.1 Hz, 1C), 27.09, 14.92 ppm. ^{19}**F NMR** (377 MHz, CDCl$_3$) δ = −65.26 ppm. **HRMS** (ESI) m/z: [M + H]$^+$ calcd for C$_{24}$H$_{24}$F$_3$N$_6$O 469.1958; found: 469.1963.

5-((1S,5R)-1-(5-(Piperidin-4-yl)-1,3,4-oxadiazol-2-yl)-5-(trifluoromethyl)-3-azabicyclo[3.1.0]hexan-3-yl)quinoline-8-carbonitrile **20**. The title compound **20** was prepared from **50** (100 mg, 0.28 mmol) and 1-(*tert*-butoxycarbonyl)piperidine-4-carboxylic acid (69 mg, 0.30 mmol) through the similar *Procedure* for the synthesis of **18**, and purified by flash column chromatography ($V_{\text{Dichloromethane}}/V_{\text{Methanol}}$ = 5:1). (35 mg, 28% yield for two steps, white solid). ^{1}**H NMR** (400 MHz, DMSO-d_6) δ = 9.06−8.99 (m, 1H), 8.71−8.65 (m, 1H), 8.19 (d, J = 8.1 Hz, 1H), 7.62 (dd, J = 8.6, 4.2 Hz, 1H), 7.33 (d, J = 8.2 Hz, 1H), 4.19 (d, J = 10.2 Hz, 1H), 4.08 (d, J = 10.4 Hz, 1H), 4.05 (d, J = 10.5 Hz, 1H), 3.92 (d, J = 10.1 Hz, 1H), 3.06 (s, 1H), 2.94 (d, J = 9.7 Hz, 2H), 2.64−2.53 (m, 2H), 2.27−2.16 (m, 2H), 1.88 (d, J = 11.5 Hz, 2H), 1.64−1.51 ppm (m, 2H). ^{13}**C NMR** (100 MHz, DMSO-d_6) δ = 169.66, 161.56, 152.07, 149.69, 148.26, 136.42, 133.88, 124.71 (q, J = 272 Hz, 1C), 121.69, 121.48, 117.96, 113.46, 104.29, 54.74, 51.53, 44.80, 35.39 (q, J = 35 Hz, 1C), 32.93, 29.63, 27.09, 14.83 ppm. ^{19}**F NMR** (377 MHz, DMSO-d_6) δ = −64.12 ppm. **HRMS** (ESI) m/z: [M + H]$^+$ calcd for C$_{23}$H$_{22}$F$_3$N$_6$O 455.1802; found: 455.1805.

5-((1S,5R)-1-(5-(4-Fluoro-1-methylpiperidin-4-yl)-1,3,4-oxadiazol-2-yl)-5-(trifluoromethyl)-3-azabicyclo[3.1.0]hexan-3-yl)quinoline-8-carbonitrile **21**. The title compound **21** was prepared from **50** (500 mg, 1.4 mmol) and 1-(*tert*-butoxycarbonyl)-4-fluoropiperidine-4-carboxylic acid (355 mg, 1.5 mmol) through the similar *Procedure* for the synthesis of **18**, and purified by flash column chromatography ($V_{\text{Dichloromethane}}/V_{\text{Methanol}}$ = 10:1). (71 mg, 10% yield for three steps, white solid). ^{1}**H NMR** (400 MHz, DMSO-d_6) δ = 9.05−9.00 (m, 1H), 8.71−8.66 (m, 1H), 8.20 (d, J = 8.1 Hz, 1H), 7.63 (dd, J = 8.6, 4.2 Hz, 1H), 7.34 (d, J = 8.2 Hz, 1H), 4.22 (d, J = 10.2 Hz, 1H), 4.09 (d, J = 10.1 Hz, 2H), 3.94 (d, J = 10.0 Hz, 1H), 2.42−2.13 ppm (m, 13H). ^{13}**C NMR** (100 MHz, DMSO-d_6) δ = 165.6 (d, J = 26 Hz, 1C), 163.04, 152.09, 149.62, 148.25, 136.42, 133.85, 124.63 (q, J = 271 Hz, 1C), 121.74, 121.51, 117.93, 113.59, 104.42, 88.15 (d, J = 172 Hz, 1C), 54.71, 51.46, 50.13, 45.43, 39.71, 39.50, 39.29, 35.91(q, J = 35 Hz, 1C), 32.91−32.58(m, 1C), 27.02, 14.95 ppm. ^{19}**F NMR** (377 MHz, DMSO-d_6) δ = −64.11,73.47 ppm. **HRMS** (ESI) m/z: [M + H]$^+$ calcd for C$_{24}$H$_{23}$F$_4$N$_6$O 487.1864; found: 487.1864.

General Procedure for the Synthesis of Compounds 22−25.
2-((1S,5R)-3-Benzyl-5-(trifluoromethyl)-3-azabicyclo[3.1.0]hexan-1-yl)-5-(1-methylpiperidin-4-yl)-1,3,4-oxadiazole **53**. To a solution of **32** (10 g, 0.035 mol) in *N,N*-dimethylformamide was added 2-(7-azabenzotriazol-1-yl)-*N,N,N′,N′*-tetramethyluronium hexafluorophosphate (14.6 g, 0.039 mol), *N,N*-diisopropylethylamine (18.3 mL, 0.11 mol), and the mixture was stirred for 5 min. The reaction mixture was added 1-methylpiperidine-4-carbohydrazide **51** (50 mg, 0.13 mmol) and then stirred for 0.5 h. TLC analysis revealed that no starting materials were detected in the reaction mixture, and compound **52** was obtained. After adding Burgess reagent (26.3 g, 0.11 mmol), the mixture was stirred for 5h at 20 °C. The crude product was concentrated under reduced pressure and purified by flash column chromatography ($V_{\text{Dichloromethane}}/V_{\text{Methanol}}$ = 10:1) to afford the product **53** (8.3 g, 58% yield, yellow solid). ^{1}**H NMR** (400 MHz, DMSO-d_6) δ = 7.37−7.23 (m, 5H), 3.73 (s, 2H), 3.20 (d, J = 9.1 Hz, 1H), 3.14 (d, J = 9.0 Hz, 1H), 2.98 (d, J = 9.1 Hz, 1H), 2.95−2.88 (m, 1H), 2.82−2.73 (m, 3H), 2.22 (s, 3H), 2.19−2.06 (m, 3H), 1.99 − 1.92 (m, 3H), 1.77−1.64 (m, 2H). ^{13}**C NMR** (100 MHz, DMSO-d_6) δ = 169.04, 162.24, 137.80, 128.44, 128.28, 127.16, 124.93 (q, J = 271 Hz, 1C), 56.83, 55.02, 53.80, 51.85, 45.73, 35.63 (q, J = 34 Hz, 1C), 31.68, 28.51 (d, J = 4.9 Hz, 1C), 27.07, 14.40 ppm. ^{19}**F NMR** (377 MHz, DMSO-d_6) δ = −64.49 ppm. **HRMS** (ESI) m/z: [M + H]$^+$ calcd for C$_{21}$H$_{26}$F$_3$N$_4$O 407.2053; found: 407.2056.

2-((1S,5R)-3-Benzyl-5-(trifluoromethyl)-3-azabicyclo[3.1.0]hexan-1-yl)-5-(1-methylpiperidin-4-yl)-1,3,4-oxadiazole **54**. To a solution of **53** (8.3 g, 0.02 mol) in methanol (100 mL) was added

palladium on carbon (10 wt %, 800 mg). The reaction mixture was allowed to stir at room temperature for 12 h under a hydrogen balloon, follow by Celite filtration, then quenched with saturated aqueous ammonium chloride and extracted with dichloromethane. The organic layers were combined, washed with brine, dried over Na$_2$SO$_4$, filtered, and concentrated under reduced pressure. The crude product was purified by flash column chromatography ($V_{\text{Dichloromethane}}/V_{\text{Methanol}}$ = 10:1) to afford product **54**. (5.9 g, 94 yield, colorless oil). ^{1}**H NMR** (400 MHz, DMSO-d_6) δ= 3.28−3.02 (m, 5H), 2.95−2.85 (m, 1H), 2.73 (d, J = 11.3 Hz, 2H), 2.17 (s, 3H), 2.06 (t, J = 11.0 Hz, 2H), 1.98−1.87 (m, 3H), 1.80−1.63 ppm (m, 3H). ^{13}**C NMR** (100 MHz, DMSO-d_6) δ = 169.14, 162.82, 125.56 (q, J = 271 Hz, 1C), 53.94, 51.33, 47.99, 45.96, 38.15 (q, J = 33 Hz, 1C), 31.78, 29.38, 28.68, 12.32 ppm. ^{19}**F NMR** (377 MHz, DMSO-d_6) δ = −63.40 ppm. **HRMS** (ESI) m/z: [M + H]$^+$ calcd for C$_{14}$H$_{20}$F$_3$N$_4$O 317.1584; found: 317.1586.

2-((1S,5R)-3-(8-Methoxyquinolin-5-yl)-5-(trifluoromethyl)-3-azabicyclo[3.1.0]hexan-1-yl)-5-(1-methylpiperidin-4-yl)-1,3,4-oxadiazole **22**. To an oven-dried 10 mL round-bottom flask equipped with a stirring bar was added **54** (500 mg, 1.57 mmol), 5-bromo-8-methoxyquinoline (276 mg, 1.57 mmol), cesium carbonate (6.0 g, 11.0 mmol), and dry 1,4-dioxane (20 mL). The resultant mixture was degassed three times, and then RuPhos Pd G3 (132 mg, 0.16 mmol) was added to the reaction mixture under argon atmosphere. The reaction mixture was heated in an oil bath at 80 °C for 3 h, The resulting solution was filtered. The solvent was extracted with ethyl acetate, washed with brine, dried by anhydrous sodium sulfate, filtered, and concentrated under reduced pressure. The crude product was purified by flash column chromatography ($V_{\text{Dichloromethane}}/V_{\text{Methanol}}$ = 10:1) to afford product **22** (70 mg, 9.3% yield, white solid). ^{1}**H NMR** (400 MHz, DMSO-d_6) δ = 8.87−8.81 (m, 1H), 8.48 (dd, J = 8.5, 1.2 Hz, 1H), 7.55 (dd, J = 8.5, 4.1 Hz, 1H), 7.40 (d, J = 8.4 Hz, 1H), 7.09 (d, J = 8.4 Hz, 1H), 3.93 (s, 3H), 3.76 (d, J = 9.4 Hz, 1H), 3.72 (d, J = 9.4 Hz, 1H), 3.66 (d, J = 9.2 Hz, 1H), 3.58 (d, J = 9.2 Hz, 1H), 2.97−2.86 (m, 1H), 2.73 (d, J = 10.7 Hz, 2H), 2.53−2.45 (m, 1H), 2.20−2.13 (m, 4H), 2.04 (t, J = 10.9 Hz, 2H), 1.99−1.90 (m, 2H), 1.79−1.65 ppm (m, 2H). ^{13}**C NMR** (100 MHz, DMSO-d_6) δ = 169.29, 162.11, 152.30, 148.90, 140.14, 135.73, 131.94, 124.98 (q, J = 271 Hz, 1C), 124.80, 121.48, 116.97, 107.84, 55.69, 54.91, 53.91, 51.74, 45.94, 35.47 (q, J = 35 Hz, 1C), 31.79, 28.67 (d, J = 4.4 Hz, 1C), 27.03, 14.32. ppm. ^{19}**F NMR** (377 MHz, DMSO-d_6) δ = −64.05 ppm. **HRMS** (ESI) m/z: [M + H]$^+$ calcd for C$_{24}$H$_{27}$F$_3$N$_5$O$_2$ 474.2111; found: 474.2117.

8-((1S,5R)-1-(5-(1-Methylpiperidin-4-yl)-1,3,4-oxadiazol-2-yl)-5-(trifluoromethyl)-3-azabicyclo[3.1.0]hexan-3-yl)quinoxaline-5-carbonitrile **23**. The title compound **23** was prepared from **54** (100 mg, 0.32 mol) and 1-methylpiperidine-4-carbohydrazide (96 mg, 0.41 mol) through the similar *Procedure* for the synthesis of **22**, and purified by flash column chromatography ($V_{\text{Dichloromethane}}/V_{\text{Methanol}}$ = 10:1). (60 mg, 41% yield, white solid). ^{1}**H NMR** (400 MHz, CDCl$_3$) δ = 8.93 (d, J = 1.6 Hz, 1H), 8.76 (d, J = 1.6 Hz, 1H), 7.95 (d, J = 8.5 Hz, 1H), 6.78 (d, J = 8.6 Hz, 1H), 4.88 (d, J = 4.8 Hz, 1H), 4.85 (d, J = 4.8 Hz, 1H), 4.42 (d, J = 11.0 Hz, 1H), 4.14 (d, J = 10.9 Hz, 1H), 2.97−2.84 (m, 3H), 2.37 (d, J = 6.1 Hz, 1H), 2.31 (s, 3H), 2.20−2.03 (m, 4H), 2.03−1.89 (m, 2H), 1.77 ppm (d, J = 5.5 Hz, 1H). ^{13}**C NMR** (100 MHz, CDCl$_3$) δ = 169.75, 161.76, 148.44, 145.88, 144.52, 141.39, 136.60, 134.61, 124.25 (q, J = 272 Hz, 1C), 117.40, 110.79, 100.75, 55.36, 54.46, 52.44, 46.21, 36.36 (q, J = 36 Hz, 1C), 32.62, 28.95, 27.40, 17.63 ppm. ^{19}**F NMR** (377 MHz, CDCl$_3$) δ = −65.72 ppm. **HRMS** (ESI) m/z: [M + H]$^+$ calcd for C$_{23}$H$_{23}$F$_3$N$_7$O 470.1911; found: 470.1914.

2-((1S,5R)-3-(1,6-Dimethyl-1H-pyrazolo[3,4-b]pyridin-4-yl)-5-(trifluoromethyl)-3-azabicyclo[3.1.0]hexan-1-yl)-5-(1-methylpiperidin-4-yl)-1,3,4-oxadiazole **24**. The title compound **25** was prepared from **54** (500 mg, 1.16 mol) and 4-bromo-1,6-dimethyl-1*H*-pyrazolo[3,4-b]pyridine (261 mg, 1.16 mol) through the similar *Procedure* for the synthesis of **22**, and purified by flash column chromatography ($V_{\text{Dichloromethane}}/V_{\text{Methanol}}$ = 10:1). (93 mg, 15% yield, yellow solid). ^{1}**H NMR** (400 MHz, DMSO-d_6) δ = 8.08 (s, 1H), 6.13 (s, 1H), 4.41 (d, J = 10.0 Hz, 1H), 4.28 (d, J = 10.1 Hz, 1H), 4.22 (d, J = 10.1 Hz, 1H),

4.01 (d, J = 10.0 Hz, 1H), 3.89 (s, 3H), 3.00−2.89 (m, 1H), 2.76 (d, J = 11.1 Hz, 2H), 2.43 (s, 3H), 2.35 (d, J = 6.3 Hz, 1H), 2.19 (s, 3H), 2.08 (t, J = 10.5 Hz, 2H), 2.01−1.93 (m, 2H), 1.87 (d, J = 6.0 Hz, 1H), 1.80−1.67 ppm (m, 2H). ^{13}C NMR (100 MHz, DMSO-d_6) δ = 169.61, 161.51, 157.95, 151.91, 147.32, 131.40, 124.54 (q, J = 272 Hz, 1C), 103.16, 98.46, 53.85, 53.26, 49.60, 45.82, 35.78 (q, J = 35 Hz, 1C) 33.47, 31.74, 28.59, 27.64, 24.51, 17.72 ppm. ^{19}F NMR (377 MHz, DMSO-d_6) δ = −64.84 ppm. HRMS (ESI) m/z: [M + H]$^+$ calcd for $C_{22}H_{27}F_3N_7O$ 462.2224; found: 462.2227.

4-((1S,5R)-1-(5-(1-Methylpiperidin-4-yl)-1,3,4-oxadiazol-2-yl)-5-(trifluoromethyl)-3-azabicyclo[3.1.0]hexan-3-yl)pyrazolo[1,5-a]-pyridine-7-carbonitrile 25. The title compound **25** was prepared from **54** (500 mg, 1.16 mol) and 4-chloropyrazolo[1,5-*a*]pyridine-7-carbonitrile (281 mg, 1.16 mol) through the similar *Procedure* for the synthesis of **22**, and purified by flash column chromatography ($V_{Dichloromethane}/V_{Methanol}$ = 6:1) (90 mg, 12.4% yield, yellow solid). ^{1}H NMR (400 MHz, DMSO-d_6) δ = 8.03 (d, J = 2.4 Hz, 1H), 7.51 (d, J = 8.3 Hz, 1H), 7.17 (d, J = 2.5 Hz, 1H), 6.22 (d, J = 8.4 Hz, 1H), 4.51 (d, J = 10.4 Hz, 1H), 4.33 (t, J = 10.8 Hz, 2H), 4.10 (d, J = 10.3 Hz, 1H), 2.96−1.86 (m, 1H), 2.71 (d, J = 10.7 Hz, 2H), 2.34 (d, J = 6.3 Hz, 1H), 2.14 (s, 3H), 2.06−1.89 (m, 5H), 1.78−1.65 ppm (m, 2H). ^{13}C NMR (100 MHz, DMSO-d_6) δ = 169.71, 161.37, 142.64, 140.52, 132.46, 124.47 (q, J = 272 Hz, 1C), 124.03, 114.47, 101.25, 101.18, 100.95, 53.98, 53.80, 50.42, 46.04, 35.62 (q, J = 35 Hz, 1C) 31.90, 28.77, 27.59, 17.44 ppm. ^{19}F NMR (377 MHz, DMSO-d_6) δ = −64.84 ppm. HRMS (ESI) m/z: [M + H]$^+$ calcd for $C_{22}H_{23}F_3N_7O$ 458.1911; found: 458.1912.

■ ASSOCIATED CONTENT

(SI) Supporting Information

The Supporting Information is available free of charge at https://pubs.acs.org/doi/10.1021/acs.jmedchem.5c00656.

> ADME profile of **19**; ameliorates kidney enlargement in the BXSB/MpJ animal model of **19**; kidney histopathological score in BXSB/MpJ mouse model of **19** and **M5049**; the binding affinities of **19** to TLR7 and TLR8; molecular docking of **19** with TLR8 and TLR7; in vitro toxicity studies of **19** and **M5049**; h-PBMC IL-6 inhibition of **19**; X-ray crystallographic analysis of **43**; HRMS and NMR spectra of all compounds; HPLC spectra of compounds **5−25** and chair HPLC spectra of compounds **31−32** (PDF)
>
> Molecular formula strings of compounds **5−25** and data (CSV)
>
> Crystal structure of **43** (CIF)
>
> Molecular docking of compound **7** with TLR8 (PDB)
>
> Molecular docking of compound **9** with TLR8 (PDB)
>
> Molecular docking of compound **10** with TLR8 (PDB)
>
> Molecular docking of compound **19** with TLR8 (PDB)
>
> Molecular docking of compound **19** with TLR7 (PDB)

■ AUTHOR INFORMATION

Corresponding Author

Yonggang Wei − *Kangbaida (Sichuan) Biotechnology Co., Ltd., Chengdu 610213, China;* ⊙ orcid.org/0000-0002-2978-3681; Email: ygwei1982@126.com

Authors

Yonghai Yuan − *Kangbaida (Sichuan) Biotechnology Co., Ltd., Chengdu 610213, China*

Zhilong Jia − *Kangbaida (Sichuan) Biotechnology Co., Ltd., Chengdu 610213, China*

Hongzhu Chu − *Kangbaida (Sichuan) Biotechnology Co., Ltd., Chengdu 610213, China*

Dejiang Kong − *Kangbaida (Sichuan) Biotechnology Co., Ltd., Chengdu 610213, China*

Feiquan Lei − *Kangbaida (Sichuan) Biotechnology Co., Ltd., Chengdu 610213, China*

Fei Ye − *Kangbaida (Sichuan) Biotechnology Co., Ltd., Chengdu 610213, China*

Xinying Qian − *Kangbaida (Sichuan) Biotechnology Co., Ltd., Chengdu 610213, China*

Jing Zhang − *Kangbaida (Sichuan) Biotechnology Co., Ltd., Chengdu 610213, China*

Xibing Zhou − *Kangbaida (Sichuan) Biotechnology Co., Ltd., Chengdu 610213, China*

Xinying Zhu − *Kangbaida (Sichuan) Biotechnology Co., Ltd., Chengdu 610213, China*

Zhiyong Li − *Kangbaida (Sichuan) Biotechnology Co., Ltd., Chengdu 610213, China*

Xueya Liang − *Kangbaida (Sichuan) Biotechnology Co., Ltd., Chengdu 610213, China*

Wei Chen − *Kangbaida (Sichuan) Biotechnology Co., Ltd., Chengdu 610213, China*

Complete contact information is available at:
https://pubs.acs.org/10.1021/acs.jmedchem.5c00656

Author Contributions

The manuscript was written through contributions of all authors. All authors have given approval to the final version of the manuscript. Authors will release the atomic coordinates upon article publication.

Notes

The authors declare no competing financial interest.

■ ABBREVIATIONS USED

anti-dsDNA, antidouble-stranded DNA; anti-Ribop, antiribosomal P; Burgess reagent, (methoxycarbonylsulfamoyl)-triethylammonium hydroxide inner salt; DIPEA, *N,N*-diisopropylethylamine; DMF, *N,N*-dimethylacetamide; DMSO, dimethyl sulfoxide; EtOAc, ethyl acetate; Et$_3$N, triethylamine; IFNs, type I interferons; HATU, 2-(7-Azabenzotriazol-1-yl)-*N,N,N′,N′*-tetramethyluronium hexafluorophosphate; IRF, interferon regulatory factor; IL-6, interleukin-6; i.p., intraperitoneal; KO, knockout; MALB, microalbumin; MALB/CREA, microalbumin-to-creatinine ratio; MeOH, methanol; NF-B, nuclear factor-kappa B; PAMPs, pathogen-associated molecular patterns; pDCs, plasmacytoid dendritic cells; PD, pharmacodynamics; PK, pharmacokinetics; PRRs, pattern recognition receptors; R848, Resiquimod; Ruphos Pd G3, (2′-amino-2-biphenylyl)(methanesulfonato-κO)palladium-dicyclohexyl(2′,6′-diisopropoxy-2-biphenylyl)phosphine (1:1); SLE, systemic lupus erythematosus; SOCl$_2$, thionyl chloride; *t*-BuOK, potassium *tert*-butoxide; TFA, trifluoroacetic acid; THF, tetrahydrofuran; TLR, Toll-like receptor; TLRs, Toll-like receptors; UTP, urinary total protein

■ REFERENCES

(1) Akira, S.; Uematsu, S.; Takeuch, O. Pathogen recognition and innate immunity. *Cell* **2006**, *124*, 783−801.

(2) Kawai, T.; Akira, S. Toll-like receptors and their crosstalk with other innate receptors in infection and immunity. *Immunity* **2011**, *34*, 637−650.

(3) Gay, N. J.; Symmons, M. F.; Gangloff, M.; Bryant, C. E. Assembly and localization of toll-like receptor signalling complexes. *Nat. Rev. Immunol.* **2014**, *14*, 546−558.

(4) West, A. P.; Koblansky, A. A.; Ghosh, S. Recognition and signaling by toll-like receptors. *Annu. Rev. Cell Dev. Biol.* **2006**, *22*, 409−437.

(5) O'Neill, L. A. J.; Golenbock, D.; Bowie, A. G. The history of toll-like receptors-redefining innate immunity. *Nat. Rev. Immunol.* **2013**, *13*, 453−460.

(6) Gorden, K. B.; Gorski, K. S.; Gibson, S. J.; Kedl, R. M.; Kieper, W. C.; Qiu, X.; Tomai, A.; Alkan, S. S.; Vasilakos, J. P. Synthetic TLR agonists reveal functional differences between human TLR7 and TLR8. *J. Immunol.* **2005**, *174*, 1259−1268.

(7) Bender, A. T.; Tzvetkov, E.; Pereira, A.; Wu, Y.; Kasar, S.; Przetak, M. M.; Vlach, J.; Niewold, T. B.; Jensen, M. A.; Okitsu, S. L. TLR7 and TLR8 differentially activate the IRF and NF-*κ*B pathways in specific cell types to promote inflammation. *Immunohorizons* **2020**, *4*, 93−107.

(8) Marshak-Rothstein, A. Toll-like receptors in systemic auto-immune disease. *Nat. Rev. Immunol.* **2006**, *6*, 823−835.

(9) Lee, Y. H.; Choi, S. J.; Ji, J. D.; Song, G. G. Association between toll-like receptor polymorphisms and systemic lupus erythematosus: a meta-analysis update. *Lupus* **2016**, *25*, 1−9.

(10) Subramanian, S.; Tus, K.; Li, Q. Z.; Wang, A.; Tian, X. H.; Zhou, J.; Liang, C.; Bartov, G.; McDaniel, L. D.; Zhou, X. J.; Schultz, R. A.; Wakeland, E. K. A Tlr7 translocation accelerates systemic autoimmunity in murine lupus. *Proc. Natl. Acad. Sci. U.S.A.* **2006**, *103*, 9970−9975.

(11) Deane, J. A.; Pisitkun, P.; Barrett, R. S.; Feigenbaum, L.; Town, T.; Ward, J. M.; Flavell, R. A.; Bolland, S. Control of toll-like receptor 7 expression is essential to restrict autoimmunity and dendritic cell proliferation. *Immunity* **2007**, *27*, 801−810.

(12) Fairhurst, A.-M.; Hwang, S.-H.; Wang, A.; Tian, X.-H.; Boudreaux, C.; Zhou, X. J.; Casco, J.; Li, Q.-Z.; Connolly, J. E.; Wakeland, E. K. Yaa autoimmune phenotypes are conferred by overexpression of TLR7. *Eur. J. Immunol.* **2008**, *38*, 1971−1978.

(13) Lee, P. Y.; Kumagai, Y.; Li, Y.; Takeuchi, O.; Yoshida, H.; Weinstein, J.; Kellner, E. S.; Nacionales, D.; Barker, T.; Kelly-Scumpia, K.; Rooijen, N.; Kumar, H.; Kawai, T.; Satoh, M.; Akira, S.; Reeves, W. H. TLR7-dependent and Fc*γ*R-independent production of type I interferon in experimental mouse lupus. *J. Exp. Med.* **2008**, *205*, 2995−3006.

(14) Savarese, E.; Steinberg, C.; Pawar, R. D.; Reindl, W.; Akira, S.; Anders, H.-J.; Krug, A. Requirement of toll-like receptor 7 for pristane-induced production of autoantibodies and development of murine lupus nephritis. *Arthritis Rheum.* **2008**, *58*, 1107−1115.

(15) Brown, G. J.; Cañete, P. F.; Wang, H.; Medhavy, A.; Bones, J.; Roco, J. A.; He, Y.; Qin, Y.; Cappello, J.; Ellyard, J. I.; Bassett, K.; Shen, Q.; Burgio, G.; Zhang, Y.; Turnbull, C.; Meng, X.; Wu, P.; Cho, E.; Miosge1, L. A.; Andrews, T. D.; Field, M. A.; Tvorogov, D.; Lopez, A. F.; Babon, J. J.; López, C. A.; Gónzalez-Murillo, Á.; Garulo, D. C.; Pascual, V.; Levy, T.; Mallack, E. J.; Calame, D. G.; Lotze, T.; Lupski, J. R.; Ding, H.; Ullah, T. R.; Walters, G. D.; Koina, M. E.; Cook, M. C.; Shen, N.; Collantes, C. L.; Corry, B.; Gantier, M. P.; Athanasopoulos, V.; Vinuesa, C. G. TLR7 gain-of-function genetic variation causes human lupus. *Nature* **2022**, *605*, 349−356.

(16) Barrat, F. J.; Meeker, T.; Gregorio, J.; Chan, J. H.; Uematsu, S.; Akira, S.; Chang, B.; Duramad, O.; Coffman, R. L. Nucleic acids of mammalian origin canact as endogenous ligands for Toll-like receptors and may promote systemic lupus erythematosu. *J. Exp Med.* **2005**, *202*, 1131−1139.

(17) Marshak-Rothstein, A.; Rifkin, I. R. Immunologically active autoantigens: the role of toll-like receptors in the development of chronic inflammatory disease. *Annu. Rev. Immunol.* **2007**, *25*, 419−441.

(18) Christensen, S. R.; Shupe, J.; Nickerson, K.; Kashgarian, M.; Flavell, R. A.; Shlomchik, M. J. Toll-like receptor 7 and TLR9 dictate autoantibody specificity and have opposing inflammatory and regulatory roles in a murine model of lupus. *Immunity* **2006**, *25*, 417−428.

(19) Nickerson, K. M.; Christensen, S. R.; Shupe, J.; Kashgarian, M.; Kim, D.; Elkon, K.; Shlomchik, M. J. TLR9 regulates TLR7-and MyD88-dependent autoantibody production and disease in a murine model of lupus. *J. Immunol* **2010**, *184*, 1840−1848.

(20) Liu, J.; Xu, C.; Hsu, L.-C.; Luo, Y.; Xiang, R.; Chuang, T.-H. A five-amino-acid motif in the undefined region of the TLR8 ectodomain is required for species-specific ligand recognition. *Mol. Immunol.* **2010**, *47*, 1083−1090.

(21) Cervantes, J. L.; Weinerman, B.; Basole, C.; Salazar, J. C. TLR8: the forgotten relative revindicated. *Cell. Mol. Immunol.* **2012**, *9*, 434−438.

(22) Kimura, J.; Ichii, O.; Miyazono, K.; Nakamura, T.; Horino, T.; Otsuka-Kanazawa, S.; Kon, Y. Overexpression of toll-like receptor 8 correlates with the progression of podocyte injury in murine autoimmune glomerulonephritis. *Sci. Rep.* **2014**, *4*, No. 7290.

(23) Wang, T.; Song, D.; Li, X.; Luo, Y.; Yang, D.; Liu, X.; Kong, X.; Xing, Y.; Bi, S.; Zhang, Y.; Hu, T.; Zhang, Y.; Dai, S.; Shao, Z.; Chen, D.; Hou, J.; Ballestar, E.; Cai, J.; Zheng, F.; Yang, J. Y. MiR-574−5p activates human TLR8 to promote autoimmune signaling and lupus. *Cell Commun. Signaling* **2024**, *22*, 1−24.

(24) Jiang, S.; Tanji, H.; Yin, K.; Zhang, S.; Sakaniwa, K.; Huang, J.; Yang, Y.; Li, J.; Ohto, U.; Shimizu, T.; Yin, H. Rationally designed small-molecule inhibitors targeting an unconventional pocket on the TLR8 protein-protein interface. *J. Med. Chem.* **2020**, *63*, 4117−4132.

(25) Guiducci, C.; Gong, M.; Cepika, A.-M.; Xu, Z.; Tripodo, C.; Bennett, L.; Crain, C.; Quartier, P.; Cush, J. J.; Pascual, V.; Coffman, R. L.; Barrat, F. J. RNA recognition by human TLR8 can lead to autoimmune inflammation. *J. Exp. Med.* **2013**, *210*, 2903−2919.

(26) Wang, X.; Liu, Y.; Han, X.; Zou, G.; Zhu, W.; Shen, H.; Liu, H. Small molecule approaches to treat autoimmune and inflammatory diseases (Part II): Nucleic acid sensing antagonists and inhibitors. *Bioorg. Med. Chem. Lett.* **2021**, *44*, No. 128101.

(27) Vlach, J.; Bender, A. T.; Przetak, M.; Pereira, A.; Deshpande, A.; Johnson, T. L.; Reissig, S.; Tzvetkov, E.; Musil, D.; Morse, N. T.; Haselmayer, P.; Zimmerli, S. C.; Okitsu, S. L.; Walsky, R. L.; Sherer, B. Discovery of M5049: a novel selective toll-like receptor 7/8 inhibitor for treatment of autoimmunity. *J. Pharmacol Exp Ther.* **2021**, *376*, 397−409.

(28) Klopp-Schulze, L.; Gopalakrishnan, S.; Yalkinoglu, Ö.; Kuroki, Y.; Lu, H.; Goteti, K.; Krebs-Brown, A.; Filho, M. N.; Gradhand, U.; Fluck, M.; Shaw, J.; Dong, J.; Venkatakrishnan, K. Asia-inclusive global development of enpatoran: results of an ethno-bridging study, intrinsic/extrinsic factor assessments and disease trajectory modeling to inform design of a phase II multiregional clinical trial. *Clin. Pharmacol. Ther.* **2024**, *115*, 1346−1357.

(29) Port, A.; Shaw, J. V.; Klopp-Schulze, L.; Bytyqi, A.; Vetter, C.; Hussey, E.; Mammasse, N.; Ona, V.; Bachmann, A.; Strugala, D.; Reh, C.; Goteti, K. Phase 1 study in healthy participants of the safety, pharmacokinetics, and pharmacodynamics of enpatoran (M5049), a dual antagonist of toll-like receptors 7 and 8. *Pharmacol Res. Perspect.* **2021**, *9*, No. e00842.

(30) Sreekantha, R. K.; Mussari, C. P.; Dodd, D. S.; Pasunoori, L.; Hegde, S.; Posy, S. L.; Critton, D.; Ruepp, S.; Subramanian, M.; Salter-Cid, L. M.; Tagore, D. M.; Sarodaya, S.; Dudhgaonkar, S.; Poss, M. A.; Schieven, G. L.; Carter, P. H.; Macor, J. E.; Dyckman, A. J. Identification of 2-pyridinylindole-based dual antagonists of toll-like receptors 7 and 8 (TLR7/8). *ACS Med. Chem. Lett.* **2022**, *13*, 812−818.

(31) Mussari, C. P.; Dodd, D. S.; Sreekantha, R. K.; Pasunoori, L.; Wan, H.; Posy, S. L.; Critton, D.; Ruepp, S.; Subramanian, M.; Watson, A.; Davies, P.; Schieven, G. L.; Salter-Cid, L. M.; Srivastava, R.; Tagore, D. M.; Dudhgaonkar, S.; Poss, Mi. A.; Carter, P. H.; Dyckman, A. J. Discovery of potent and orally bioavailable small molecule antagonists of toll-like receptors 7/8/9 (TLR7/8/9). *ACS Med. Chem. Lett.* **2020**, *11*, 1751−1758.

(32) Betschart, C.; Faller, M.; Zink, F.; Hemmig, R.; Blank, J.; Vangrevelinghe, E.; Bourrel, M.; Glatthar, R.; Behnke, D.; Barker, K.; Heizmann, A.; Angst, D.; Nimsgern, P.; Jacquier, S.; Junt, T.; Zipfel, G.; Ruzzante, G.; Loetscher, P.; Limonta, S.; Hawtin, S.; Andre, C. B.; Boulay, T.; Feifel, R.; Knoepfel, T. Structure-based optimization of a

fragment-like TLR8 binding screening hit to an in vivo efficacious TLR7/8 antagonist. *ACS Med. Chem. Lett.* **2022**, *13*, 658−664.

(33) Alper, P.; Betschart, C.; André, C.; Boulay, T.; Cheng, D.; Deane, J.; Faller, M.; Feifel, R.; Glatthar, R.; Han, D.; Hemmig, R.; Jiang, T.; Knoepfel, T.; Maginnis, J.; Mutnick, D.; Pei, W.; Ruzzante, Gi.; Syka, P.; Zhang, G.; Zhang, Y.; Zink, F.; Zipfel, G.; Hawtin, S.; Junt, T.; Michellys, P.-Y. Discovery of the TLR7/8 antagonist MHV370 for treatment of systemic autoimmune diseases. *ACS Med. Chem. Lett.* **2023**, *14*, 1054−1062.

(34) Hawtin, S.; Andre′, C.; Collignon-Zipfel, G.; Appenzeller, S.; Bannert, B.; Baumgartner, L.; Beck, D.; Betschart, C.; Boulay, T.; Brunner, H. I.; Ceci, M.; Deane, J.; Feifel, R.; Ferrero, E.; Kyburz, D.; Lafossas, F.; Loetscher, P.; Merz-Stoeckle, C.; Michellys, P.; Nuesslein-Hildesheim, B.; Raulf, F.; Rush, J. S.; Ruzzante, G.; Stein, T.; Zaharevitz, S.; Wieczorek, G.; Siegel, R.; Gergely, P.; Shisha, T.; Junt, T. Preclinical characterization of the toll-like receptor 7/8 antagonist MHV370 for lupus therapy. *Cell Rep. Med.* **2023**, *4*, No. 101036.

(35) Ishizaka, S. T.; Hawkins, L.; Chen, Q.; Tago, F.; Yagi, T.; Sakaniwa, K.; Zhang, Z.; Shimizu, T.; Shirato, M. A novel toll-like receptor 7/8-specific antagonist E6742 ameliorates clinically relevant disease parameters in murine models of lupus. *Eur. J. Pharmacol.* **2023**, *957*, No. 175962.

(36) Yamakawa, N.; Tago, F.; Nakai, K.; Kitahara, Y.; Ikari, S.; Hojo, S.; Hall, N.; Aluri, J.; Hussein, Z.; Gevorkyan, H.; Maruyama, T.; Ishizaka, S.; Yagi, T. First-in-human study of the safety, tolerability, pharmacokinetics, and pharmacodynamics of E6742, a dual antagonist of toll-like receptors 7 and 8, in healthy volunteers. *Clin. Pharmacol. Drug Dev.* **2023**, *12*, 363−375.

(37) Wang, M.; Chena, H.; Zhang, T.; Zhang, Z.; Xiang, X.; Gao, M.; Guo, Y.; Jiang, S.; Yin, K.; Chen, M.; Huang, J.; Zhong, X.; Ohto, U.; Li, J.; Shimizu, T.; Yin, H. Targeting toll-like receptor 7 as a therapeutic development strategy for systemic lupus erythematosus. *Acta Pharm. Sin. B* **2024**, *14*, 4899−4913.

(38) Kundu, B.; Raychaudhuri, D.; Mukherjee, A.; Sinha, B. P.; Sarkar, D.; Bandopadhyay, P.; Pal, S.; Das, N.; Dey, D.; Ramarao, K.; Nagireddy, K.; Ganguly, D.; Talukdar, A. Systematic optimization of potent and orally bioavailable purine scaffold as a dual inhibitor of toll-like receptors 7 and 9. *J. Med. Chem.* **2021**, *64*, 9279−9301.

(39) Das, N.; Bandopadhyay, P.; Roy, S.; Sinha, B. P.; Dastidar, U. G.; Rahaman, O.; Pal, S.; Ganguly, D.; Talukdar, A. Development, optimization, and in vivo validation of new imidazopyridine chemotypes as dual TLR7/TLR9 antagonists through activity-directed sequential incorporation of relevant structural subunits. *J. Med. Chem.* **2022**, *65*, 11607−11632.

(40) Sun, Z.; Liu, J.; Shi, L.; Yang, M.; Wang, Y.; Han, Y.-P.; Yao, X.; Liang, Y.-M. New synthetic approaches for the construction of enantioenriched molecules bearing quaternary stereocenters. *Adv. Synth. Catal.* **2024**, *366*, 4294−4322.

(41) Wang, B.; Tu, Y. Q. Stereoselective construction of quaternary carbon stereocenters via a semipinacol rearrangement strategy. *Acc. Chem. Res.* **2011**, *44*, 1207−1222.

(42) Liu, Y.; Han, S.-J.; Liu, W.-B.; Stoltz, B. M. Catalytic enantioselective construction of quaternary stereocenters: assembly of key building blocks for the synthesis of biologically active molecules. *Acc. Chem. Res.* **2015**, *48*, 740−751.

(43) Ling, T.; Rivas, F. All-carbon quaternary centers in natural products and medicinal chemistry: recent advances. *Tetrahedron* **2016**, *72*, 6729−6777.

(44) Xu, P.; Zhou, F.; Zhu, L.; Zhou, J. Catalytic desymmetrization reactions to synthesize all-carbon quaternary stereocentres. *Nat. Synth.* **2023**, *2*, 1020−1036.

(45) Wei, W.; Cherukupalli, S.; Jing, L.; Liu, X.; Zhan, P. Fsp3: a new parameter for drug-likeness. *Drug Discovery Today* **2020**, *25*, 1839−1845.

(46) Lovering, F.; Bikker, J.; Humblet, C. Escape from flatland: increasing saturation as an approach to improving clinical success. *J. Med. Chem.* **2009**, *52*, 6752−6756.

(47) Büschleb, M.; Dorich, S.; Hanessian, S.; Tao, D.; Schenthal, K. B.; Overman, L. E. Synthetic strategies toward natural products containing contiguous stereogenic quaternary carbon atoms. *Angew. Chem., Int. Ed.* **2016**, *55*, 4156−4186.

(48) Long, R.; Huang, J.; Gong, J.; Yang, Z. Direct construction of vicinal all-carbon quaternary stereocenters in natural product synthesis. *Nat. Prod. Rep.* **2015**, *32*, 1584−1601.

(49) Song, Z.-L.; Fan, C.-A.; Tu, Y.-Q. Semipinacol rearrangement in natural product synthesis. *Chem. Rev.* **2011**, *111*, 7523−7556.

(50) Zhou, F.; Zhu, L.; Pan, B.-W.; Shi, Y.; Liu, Y.-L.; Zhou, J. Catalytic enantioselective construction of vicinal quaternary carbon stereocenters. *Chem. Sci.* **2020**, *11*, 9341−9365.

(51) Tanji, H.; Ohto, U.; Shibata, T.; Miyake, K.; Shimizu, T. Structural reorganization of the toll-like receptor 8 dimer induced by agonistic ligands. *Science* **2013**, *339*, 1426−1429.

(52) Glomb, T.; Szymankiewicz, K.; Świątek, P. Anti-cancer activity of derivatives of 1,3,4-oxadiazole. *Molecules* **2018**, *23*, No. 3361.

(53) Chawla, G.; Naaz, B.; Siddiqui, A. A. Exploring 1,3,4-oxadiazole scaffold for anti-inflammatory and analgesic activities: a review of literature from 2005−2016. *Mini-Rev. Med. Chem.* **2018**, *18*, 216−233.

(54) Vaidya, A.; Pathak, D.; Shah, K. 1,3,4-Oxadiazole and its derivatives: A review on recent progress in anticancer activities. *Chem. Biol. Drug Des.* **2021**, *97*, 572−591.

(55) Tiwari, D.; Narang, R.; Sudhakar, K.; Singh, V.; Lal, S.; Devgun, M. 1,3,4-Oxadiazole derivatives as potential antimicrobial agents. *Chem. Biol. Drug. Des.* **2022**, *100*, 1086−1121.

(56) Lee, E. C.; Hong, B. H.; Lee, J. Y.; Kim, J. C.; Kim, D.; Kim, Y.; Tarakeshwar, P.; Kim, K. S. Substituent effects on the edge-to-face aromatic interactions. *J. Am. Chem. Soc.* **2005**, *127*, 4530−4537.

(57) Martin, L. J.; Koegl, M.; Bader, G.; Cockcroft, X.-L.; Fedorov, O.; Fiegen, D.; Gerstberger, T.; Hofmann, M. H.; Hohmann, A. F.; Kessler, D.; Knapp, S.; Knesl, P.; Kornigg, S.; Müller, S.; Nar, H.; Rogers, C.; Rumpel, K.; Schaaf, O.; Steurer, S.; Tallant, C.; Vakoc, C. R.; Zeeb, M.; Zoephel, A.; Pearson, M.; Boehmelt, G.; McConnell, D. Structure-based design of an in vivo active selective BRD9 inhibitor. *J. Med. Chem.* **2016**, *59*, 4462−4475.